isomer but only 80% pure. Further purification by preparative GC employing the same column but with the GC oven chamber cooled with dry ice to temperatures ranging from -30 to -15 °C (retention time: 100 min) gave 35 mg of (-)-(1*S*,2*R*,3*R*)-*c*-**1** (93.3% pure by analytical GC; two impurities, 2.0 and 4.7%, possibly ethylcyclobutane-d_3 and *n*-propylcyclopropane-d_3[31]): ^{1}H NMR δ 1.32-1.24 (q, J = 7.3 Hz, 2 H), 1.00 (s, 3 H), 0.97 (t, J = 4.8 Hz, 3 H), -0.37 (s, 1 H); uncorrected specific rotations $[\alpha]_D$ -20.5°, $[\alpha]_{365}$ -67.4° (*c* 0.8, $CDCl_3$); corrected specific rotations $[\alpha]_D$ -21.5°, $[\alpha]_{365}$ -72.5° (*c* 0.8, $CDCl_3$); mass spectrum *m/e* 87 (M^+, 33), 72 (28), 71 (14), 59 (20), 58 (77), 57 (59), 56 (29), 44 (65), 43 (100), 42 (57), 41 (34), 40 (41).

The small amount of (+)-(1*S*,2*S*,3*R*)-*t*-**1** material present in the crude product mixture was collected from the same GC runs (at room temperature) in a purity of >98.5%: $[\alpha]_D$ +40.4°, $[\alpha]_{365}$ +121° (*c* 0.62, $CDCl_3$).

Thermal Isomerizations of (±)-*t*-1, (-)-(1*R*,2*R*,3*S*)-*t*-1, and (-)-(1*S*,2*R*,3*R*)-*c*-1. All kinetics runs were carried out in a static gas-phase reactor at 380 °C. Thermolyses using (±)-*t*-**1** and (-)-(1*R*,2*R*,3*S*)-*t*-**1** were run with neat samples. The pressure in the reactor during these runs was between 103 and 122 Torr, while the sample amount per run ranged from 55.4 to 65.9 mg. Due to the small amount of sample available, the kinetic run with (-)-(1*S*,2*R*,3*R*)-*c*-**1** included added pentane as an inert bath-gas to attain the desired pressure in the kinetic bulb. About 26 mg of (-)-(1*S*,2*R*,3*R*)-*c*-**1** combined with 27 mg of pentane resulted in a pressure of 109 Torr in the bulb. The pentane used was purified by treatment with aqueous potassium permanganate solution to remove traces of olefins, followed by heating at reflux over sodium and then by distillation from sodium; preparative GC of the distilled material gave pentane with a purity of 100%, according to capillary GC analyses.

All reactants were subjected to two freeze-thaw cycles prior to introduction into the vacuum line to ensure correct pressure readings and efficient vacuum transfers. Capillary GC analyses of the recovered thermolysis product mixtures were carried out for each kinetic point by performing three 1-μL injections of neat material. The products were then separated into their cis and trans isomer sets by preparative GC on a 4.6-m 20% SP-2100 on 60/80 Chromosorb-W HP column at room temperature; the separate sets of geometric isomers were analyzed by ^{1}H NMR in $CDCl_3$ solutions (99.8 atom % D, containing no Me_4Si), as exemplified in Figures 1 and 2. The cis and trans products resulting from kinetic runs with chiral starting materials were further characterized by polarimetric measurements. For each of these determinations, a neat sample from preparative GC collections was drawn into a microsyringe and delivered to a 1-mL volumetric flask. The weight of sample transferred to the flask was measured, and the sample was diluted with $CDCl_3$ to give the 1-mL solution used for the polarimetry. The relevant data are gathered in Table V. Given uncertainties in sample weights of ±0.1 mg and in observed rotations of ±0.001°, specific rotations for very small samples showing very low rotations have significant relative uncertainties. Analyses for the thermolysis products from (±)-*t*-**1**, (-)-(1*R*,2*R*,3*S*)-*t*-**1**, and (-)-(1*S*,2*R*,3*R*)-*c*-**1** are summarized in Tables I, II, and III.

(31) The ^{1}H NMR spectrum for *n*-propylcyclopropane in CCl_4 has been reported: Kamyshova, A. A.; Chukovskaya, E. Ts.; Freidlina, R. Kh. *Proc. Acad. Sci. USSR, Chem. Sect.* **1977**, *233*, 112-115; *Dokl. Akad. Nauk SSSR* **1977**, *233*, 122-125.

Acknowledgment. We thank the National Science Foundation for support of this work through CHE 87-21656 and CHE 91-00246.

The Type 2 Intramolecular Imino Diels-Alder Reaction. Synthesis and Structural Characterization of Bicyclo[*n*.3.1] Bridgehead Olefin/Bridgehead Lactams

Timothy G. Lease and K. J. Shea*

Contribution from the Department of Chemistry, University of California, Irvine, Irvine, California 92717. *Received October 13, 1992*

Abstract: The type 2 imino Diels-Alder cycloaddition was used for the synthesis of a homologous series of bridgehead olefin/bridgehead lactams. The X-ray crystal structures of three members of this series, including the highly strained 2-carbomethoxy-8-oxo-2-azabicyclo[3.3.1]non-4-ene, were obtained. An analysis of the structural data permits evaluation of the responses of the bridgehead double bond and bridgehead amide linkages to similar torsional distortions.

Introduction

Bridgehead olefins **1** represent one class of molecules that contain a distorted double bond.[1] The topologic constraints of bridged bicyclic molecules force a double bond emanating from the bridgehead position to deviate from the preferred planar geometry. One result of the distortion is reduced overlap of the p-orbitals comprising the π-bond. The key substructural unit of a bridgehead olefin is the *trans*-cycloalkene. As the size of the *trans*-cycloalkene ring is reduced, the olefin becomes more distorted.

1

Chemists have been interested in bridgehead olefins since Bredt studied a series of naturally occurring bicyclic terpenes in the 1920s and concluded that it was not possible to locate an olefin at the bridgehead position.[2] Despite "Bredt's Rule", many bridgehead olefins have been synthesized. However, relatively few have been structurally characterized so that the details of the double bonds' distortions could be understood.

Bridgehead lactams **2** are another class of anti-Bredt molecules.[3] The bridgehead imine bond of the zwitterionic resonance form

(1) Bridgehead olefin reviews: (a) Warner, P. M. *Chem. Rev.* **1989**, *89*, 1067-1093. (b) Wentrup, C. *Reactive Molecules*; John Wiley and Sons: New York, 1984; pp 265-308. (c) Szeimies, G. In *Reactive Intermediates*; Abranovitch, R. A., Ed.; Plenum: New York, 1983; Vol. 3, pp 299-366. (d) Shea, K. J. *Tetrahedron* **1980**, *36*, 1683-1715. (e) Lease, T. G.; Shea, K. J. In *Advances in Theoretically Interesting Molecules*; Thummel, R. P., Ed.; JAI: Greenwich, CT, 1992; Vol. 2, pp 79-112. (f) Keese, R.; Luef, W. In *Topics in Stereochemistry*; Eliel, E. L., Wilen, S. H., Eds.; J. Wiley & Sons: New York, 1991; Vol. 20, pp 231-318. (g) Broden, W. T. *Chem. Rev.* **1989**, *89*, 1099.

(2) Bredt, J. *Liebigs Ann. Chem.* **1924**, *437*, 1-13.

(3) (a) Lukes, R. *Collect. Czech. Chem. Commun.* **1938**, *10*, 148. For reviews of bridgehead lactams see: (b) Greenberg, A. In *Structure and Reactivity*; Liebman, J. F., Greenberg, A., Eds.; VCH: New York, 1988; Vol. 7, Chapter 4. (c) Hall, H. K., Jr.; El-Shekeil, A. *Chem. Rev.* **1983**, *83*, 549-555.

0002-7863/93/1515-2248$04.00/0

2z is analogous to a bridgehead olefin: the amide is planar in the ground state and will therefore be destabilized when incorporated at the bridgehead position of a bicyclic molecule. The destabilization, in the form of reduced overlap of the nitrogen lone pair orbital with the carbonyl π-system, comes at the expense of the estimated 17-21 kcal/mol resonance stabilization of amides.[4] In analogy to bridgehead olefins, the strain of bridgehead lactams is expected to increase as the size of the *trans*-lactam ring is reduced.

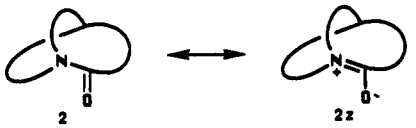

2 2z

The resonance stabilization energy corresponds to the cis–trans isomerization barrier in amides. Distorted bridgehead lactams may therefore be considered as models for species along the reaction coordinate of the cis–trans amide interconversion. They may also serve as models for amide activation in biological systems. The biological importance of distorted amides as transition-state analogs for in vivo peptide cleavage has resulted in recent theoretical[5] and experimental[6] investigations of amide excited states.

The type 2 intramolecular Diels–Alder cycloaddition has been developed as an efficient synthetic entry to [*n*.3.1] bridgehead olefins (eq 1).[7] Although heteroatoms had been included in the tether or peripheral substituents of several type 2 intramolecular Diels–Alder cycloaddition substrates, only all-carbon dienes and dienophiles had been employed prior to this study. We recognized a considerable synthetic potential to produce heterocycles by including heteroatoms in the diene or dienophile.

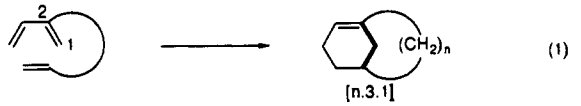

[n.3.1] (1)

Application of the type 2 intramolecular imino Diels–Alder reaction was envisioned as a synthetic entry to a class of structurally novel compounds which possess not only a bridgehead olefin but also a bridgehead amide (eq 2). Determination of the structure of the cycloadducts would permit evaluation of the response of the olefin to the strain of occupying the bridgehead position of the bicyclic framework. Variation of the diene–dienophile tether length would allow examination of the change in distortions of the olefin as the *trans*-cycloalkene ring size was varied.

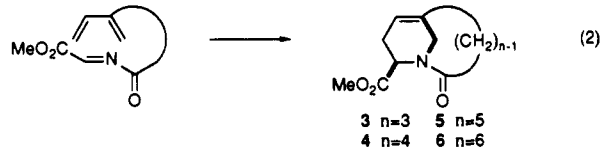

3 n=3 5 n=5
4 n=4 6 n=6 (2)

The lactam linkage was expected to experience similar distortions: the cycloadducts would resemble an unstrained lactam **8** when the diene–dienophile tether was sufficiently long; but the amino ketone resonance form **7** was expected to dominate when the tether length did not permit the geometry required for effective overlap of the nitrogen lone pair with the carbonyl group. We therefore anticipated the opportunity to observe the transition from lactam to amino ketone as the hydrocarbon tether was shortened.

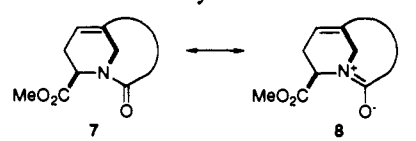

7 8

(4) Kamei, H. *Bull. Chem. Soc. Jpn.* **1968**, *41*, 2269.
(5) Li, Y.; Garrell, R. L.; Houk, K. N. *J. Am. Chem. Soc.* **1991**, *113*, 5895–5896.
(6) Song, S.; Asher, S. A.; Krimm, S.; Shaw, K. D. *J. Am. Chem. Soc.* **1991**, *113*, 1155.
(7) (a) Shea, K. J.; Wise, S.; Burke, L. D.; Davis, P. D.; Gilman, J. W.; Greeley, A. C. *J. Am. Chem. Soc.* **1982**, *104*, 5708–5715. (b) Shea, K. J.; Wada, E. *J. Am. Chem. Soc.* **1982**, *104*, 5715–5719. (c) Shea, K. J.; Wise, S. *Tetrahedron Lett.* **1979**, 1011–1014.

Scheme I

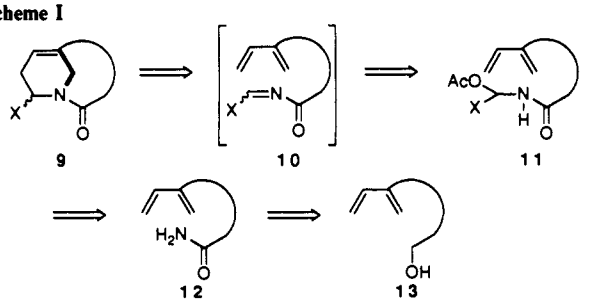

9 10 11 12 13

Table I. Diels–Alder Cycloadditions of Acetoxy Amides **22a–d**

n	substrate	cycloadduct	temp (°C)	time	% yield
3	**22a**	**3**	252	2.50 min	29
4	**22b**	**4**	200	2.0 h	82
5	**22c**	**5**	215	2.0 h	76
6	**22d**	**6**	307	5.0 min	9

This report details the synthesis of [*n*.3.1] bridgehead olefin/bridgehead lactams **3–6** by the type 2 intramolecular imino Diels–Alder reaction. The X-ray crystal structure determination of the homologous series of anti-Bredt molecules and a detailed analysis of the distortions of the two functional groups are described.[8]

Results and Discussion

Synthesis of Bridgehead Olefin/Lactams. Retrosynthetic analysis of the bicyclo[*n*.3.1] bridgehead olefin/lactams anticipated a Diels–Alder cycloadduct **9** would arise from an *N*-acyl imine **10**, which would be formed from the corresponding acetoxy amide **11** (Scheme I). The acetoxy amide was envisioned as a derivative of a 2-substituted diene amide **12** available from the corresponding diene alcohols **13**.

The use of an *N*-acyl imine as a dienophile in the Diels–Alder cycloaddition has precedent from the work of Weinreb.[9] *N*-acyl imines are extremely reactive species that can be isolated only when extensively substituted by electron-withdrawing substituents. The acyl imine therefore would be generated in situ by the thermal elimination of acetic acid from the corresponding acetoxy amide.

The diene alcohols **13** necessary to synthesize the precursors to the bicyclo[*n*.3.1] bridgehead olefin/amides where $n = 3$, 4, or 5 were known.[10] However, the diene alcohol necessary to synthesize the precursor to the [6.3.1] cycloadduct has not been reported. Synthesis of **18d** from commercially available 1,6-hexanediol is outlined below.

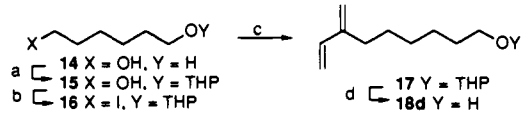

a **14** X = OH, Y = H
b **15** X = OH, Y = THP
b **16** X = I, Y = THP
d **17** Y = THP
d **18d** Y = H

(a) dihydropyran, HCl (cat.) (b) 1. MsCl, NEt_3 2. NaI (c) CH_2=CHC(MgCl)=CH_2.[11] Li_2CuCl_4 (cat.)[12] (d) EtOH, PPTS (cat.)[13]

(8) A portion of this work has appeared in preliminary form: Shea, K. J.; Lease, T. G.; Ziller, J. W. *J. Am. Chem. Soc.* **1990**, *112*, 8627–8629.
(9) (a) Melnick, M. J.; Weinreb, S. M. *J. Org. Chem.* **1988**, *53*, 850–854. (b) Weinreb, S. M. *Acc. Chem. Res.* **1985**, *18*, 16–21. (c) Bailey, T. R.; Garigipati, R. S.; Morton, J. A.; Weinreb, S. M. *J. Am. Chem. Soc.* **1984**, *106*, 3240–3245. (d) Bremmer, M. L.; Khatri, N. A.; Weinreb, S. M. *J. Org. Chem.* **1983**, *48*, 3661–3666. (e) Bremmer, M. L.; Weinreb, S. M. *Tetrahedron Lett.* **1983**, *24*, 261–264. (f) Gobao, R. A.; Bremmer, M. L.; Weinreb, S. M. *J. Am. Chem. Soc.* **1982**, *104*, 7065–7068. (g) Khatri, N. A.; Schmitthenner, H. F.; Shringapure, J.; Weinreb, S. M. *J. Am. Chem. Soc.* **1981**, *103*, 6387–6393. (h) Nader, B.; Bailey, T. R.; Franck, R. W.; Weinreb, S. M. *J. Am. Chem. Soc.* **1981**, *103*, 7573–7580. (i) Schmitthenner, H. F.; Weinreb, S. M. *J. Org. Chem.* **1980**, *45*, 3372–3373. (j) Nader, B.; Franck, R. W.; Weinreb, S. M. *J. Am. Chem. Soc.* **1980**, *102*, 1153–1155.
(10) Shea, K. J.; Burke, L. D. *J. Org. Chem.* **1988**, *53*, 318–327.
(11) Nunomoto, S.; Yamashita, Y. *J. Org. Chem.* **1979**, *44*, 4788–4791.
(12) Nunomoto, S.; Kawakami, Y.; Yamashita, Y. *J. Org. Chem.* **1983**, *48*, 1912–1914.
(13) Sterzycki, R. *Synthesis* **1979**, 724–725. Miyashita, M.; Yoshikoshi, A.; Grieco, P. A. *J. Org. Chem.* **1977**, *42*, 3772–3774.

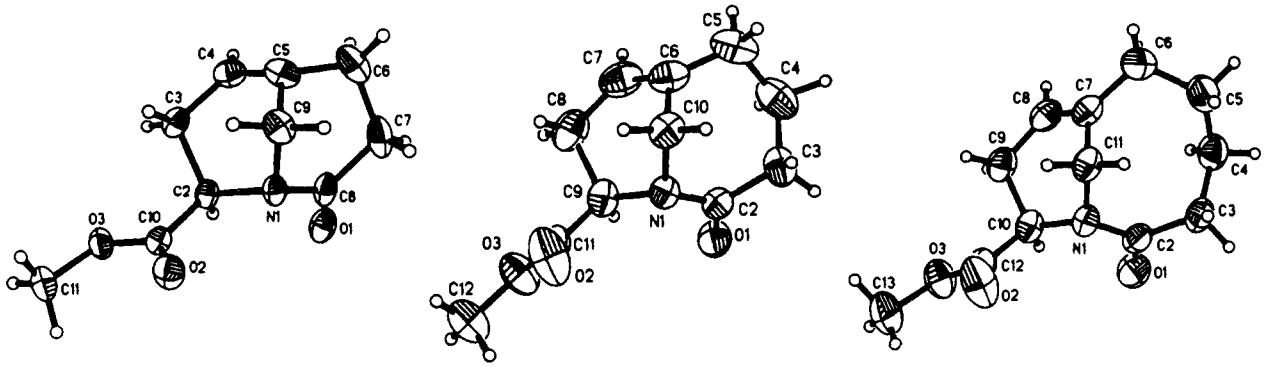

3 4 5

Figure 1. ORTEP plots of Diels–Alder cycloadducts 3, 4, and 5.

Diels–Alder cycloaddition precursors **22a–d** were prepared from the corresponding diene alcohols. Oxidation of alcohols **18b–d** by pyridinium dichromate (PDC)[14] afforded the corresponding diene acids **19b–d**. Diene acid **19a** was prepared as reported previously.[10] The acids were converted to the corresponding amides by treatment with oxalyl chloride[15] followed by addition of ammonia. The amides **20a–d** were condensed[9h] with methyl glyoxalate[16] to yield the corresponding methyl alcohols **21a–d**. Finally, the methyl alcohols were acetylated using acetic anhydride/pyridine to afford the acetates **22a–d**, the Diels–Alder cycloaddition precursors.

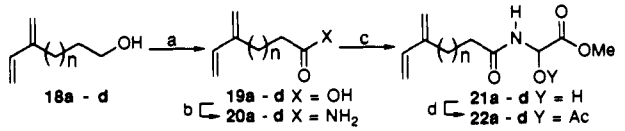

(a) PDC (b) 1. $(COCl)_2$ 2. NH_3 (c) MeO_2CCHO (d) Ac_2O, pyridine

Diels–Alder Cycloaddition Reactions. Bridgehead olefin/amides **3–6** were prepared by the type 2 intramolecular Diels–Alder cycloaddition of acetoxy amides **22a–d**, respectively (Table I).

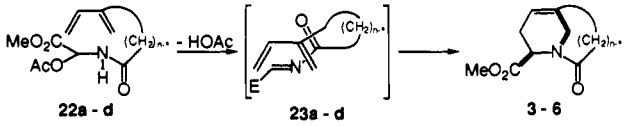

Thermolysis of dilute solutions of the acetoxy amides (0.01 M in xylenes) afforded the corresponding cycloadducts. The intermediacy of the *N*-acyl imines **23a–d** is inferred from the structure of the cycloadducts; however, no attempt was made to either isolate or spectroscopically observe the intermediates. The bridgehead olefins **3–6** were purified by silica gel chromatography to give colorless solids. Compounds **3–5** were crystalline and were analyzed by X-ray crystallography (Figure 1).[17]

The type 2 intramolecular Diels–Alder reaction normally affords bicyclo[*n*.3.1]alkenes via a reactive conformation such as **23**.[18] The alternative regiochemical orientation of the diene relative to the dienophile would proceed via a conformation such as **24** to give bicyclo[*n*.2.2]alkenes **25**. These are not observed in the cycloadditions of *N*-acyl imines **23** primarily because the tether is too short to permit effective diene–dienophile orbit overlap.

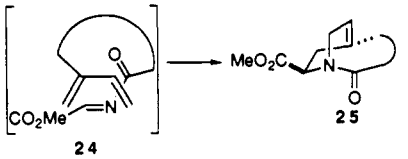

24 25

The Diels–Alder reaction is presumed to proceed through a transition state in which the diene–dienophile tether occupies an endo position. Transition state **26**, in which the tether occupies

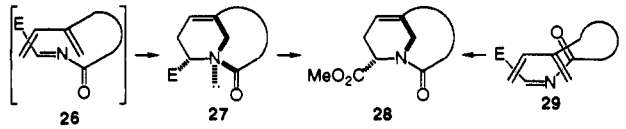

26 27 28 29

an exo position, would produce cycloadduct **27**, in which the nitrogen lone pair would be inside the bicyclic skeleton of the product. Such "inside-outside" bicyclic molecules, in which a proton (instead of a lone pair of electrons) is held within the bicyclic framework, are higher in energy than their "right-side-out" isomers. Product **27** would presumably invert to its homeomorphic isomer **28**; but no product containing the carbomethoxy group in the endo position (as in **28**) is observed in the cycloadditions. Previous experience with the type 2 intramolecular Diels–Alder reaction in which no "inside-outside" products have been isolated and the failure to observe cycloadducts **28** (assuming the *E*-acyl imine **26** and not the *Z*-acyl imine is present in the transition state, vide infra) suggests the tether is in the endo position in the transition state.

(14) Corey, E. J.; Schmidt, G. *Tetrahedron Lett.* **1979**, 399–402.
(15) Burgstahler, A. W.; Weigel, L. O.; Shaefer, C. G. *Synthesis* **1976**, 767–768.
(16) Kelly, T. R.; Schmidt, T. E.; Haggerty, J. G. *Synthesis* **1972**, 544–545.

(17) The X-ray crystal structure of **3** has been reported.[8] X-ray diffraction data for **4** and **5**: The crystals belong to the monoclinic system with unit cell parameters at 296 K given below.

compd no.	**4**	**5**
emp form	$C_{11}H_{15}NO_3$	$C_{12}H_{17}NO_3$
a (Å)	12.5065(15)	19.693(9)
b (Å)	6.6167(7)	8.128(2)
c (Å)	13.115(2)	7.123(2)
β (deg)	101.270(11)	92.15(3)
V (Å^3)	1064.4(2)	1139.4(7)
density$_{calc}$ (mg/m^3)	1.306	1.302
refls colltd	2154	2904
ind refls ($\|F_o\| < 0$)	1749 (R_{int} = 0.92%)	2382 (R_{int} = 1.4%)
obsd refls ($\|F_o\| > 4.0\sigma(\|F_o\|)$)	1482	1885
final *R* indices (obsd data)	R_F = 4.1%, R_{wF} = 5.9%	R_F = 4.1%, R_{wF} = 5.6%
R indices (all data)	R_F = 5.1%, R_{wF} = 6.2%	R_F = 5.7%, R_{wF} = 7.9%
goodness-of-fit	1.96	1.72
no. of variables	197	214

The space group is $P2_1/n$ with $Z = 4$ formula units per unit cell. Intensity data were collected on a Siemens R3m/V diffractometer system using monochromatized Mo Kα radiation ($\bar{\nu}$ = 0.710730 Å) by a θ–2θ scan technique.[17a] The structures were solved by direct methods and refined by full-matrix least-squares techniques.[17b,c] Hydrogen atoms were located from a difference Fourier map and included with isotropic temperature parameters. The final difference Fourier maps were featureless. (a) Churchill, M. R.; Lashewycz, R. A.; Rotella, F. J. *Inorg. Chem.* **1977**, *16*, 265–271. (b) UCLA Crystallographic Computing Package, University of California, Los Angeles, 1981, C. Strouse, personal communication. (c) SHELXTL PLUS Program set; Siemens Analytical X-Ray Instruments, Inc.: Madison, WI, 1989.

(18) For exceptions see: (a) Beauchamp, P. S. Ph.D. Dissertation, University of California, Irvine, 1981. (b) Shea, K. J.; Staab, A. J. University of California, Irvine, unpublished results.

Alternatively, cycloadduct **28** could have arisen from reaction of the *Z*-acyl imine **29**. Cycloadducts **3–6**, in which the carbomethoxy group is anti to the tether, indicate the *E*-acyl imine **23**

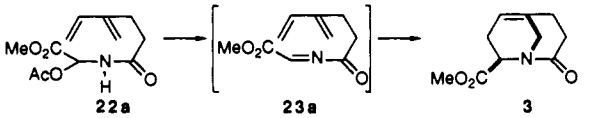

22a **23a** **3**

is formed stereoselectively in the thermolytic elimination of acetic acid from acetates **22** or, in the event of a facile *E*/*Z* interconversion, the *E* form is more reactive in the cycloaddition. These results are in agreement with Weinreb's study of the (type 1) intramolecular imino Diels–Alder cycloadditions.[9] In those experiments only products arising from the *E*-acyl imine were formed when ester-activated dienophiles were employed.

Bicyclo[3.3.1]nonene derivative **3** proved to be the most difficult bridgehead olefin/amide to synthesize and isolate. Only upon careful drying of substrate, solvents, and glassware, and preparation of the thermolysis samples under N_2 was the cycloaddition successful.

GC analysis of 0.01 M solutions of acetate **22a** heated to temperatures ranging from 200 to 320 °C revealed the starting material was completely consumed; however, cycloadduct **3** was observed by GC only at short reaction times, indicating secondary reactions are capable of consuming the primary reaction product. Preparative scale reactions were carried out at 250 °C for 2.5 min in order to completely consume **22a** (which is difficult to separate from **3**) while minimizing decomposition of the cycloadduct. Under these conditions the bicyclo[3.3.1]nonene product could be isolated in 29% yield as a colorless crystalline solid.

The strain present in the bridgehead olefin of **3** was manifest in its reactivity toward oxygen: exposure of concentrated samples of **3** to air resulted in formation of epoxide **30**.

3 **30**

Interestingly, dilute solutions of the cycloadduct were not oxidized by air nor even when oxygen gas was passed through the solution. The concentration dependence of the epoxidation may be explained by a mechanism in which there is a reversible initial addition of oxygen to the bridgehead olefin to give diradical **31** (Scheme II). In the presence of a second molecule of **3**, the diradical peroxide **32** may be formed. Intermediate **32** may then decompose to two molecules of epoxide. In the absence of a second molecule of **3**, as may be expected for a dilute solution of the cycloadduct, diradical **31** may revert to dioxygen and the bridgehead olefin.

For most purposes cycloadduct **3** could be conveniently handled under N_2 without significant decomposition to the epoxide. However the bridgehead olefin could not be recrystallized using standard Schlenk techniques. Recrystallization for the X-ray diffraction analysis was therefore carried out in a nitrogen drybox.

The difficulties encountered in preparing and handling cycloadduct **3** initially led to isolation of apparently pure samples which were not solid. One of the reasons for incorporating the ester functionality in the Diels–Alder substrate was to provide an opportunity to prepare a crystalline derivative if the ester cycloadducts were oils. Therefore, before the first crystalline samples of **3** were obtained, the methyl ester was saponified in order to obtain the carboxylic acid derivative. Addition of 5.3 equiv of LiOH to **3** in aqueous acetonitrile led to complete consumption of the ester within 1 h. Carboxylic acid **33** could be isolated as a colorless amorphous solid in 46% yield. The low yield may be due to addition of acid or water to the bridgehead olefin, or nucleophilic addition of water to the lactam.[19]

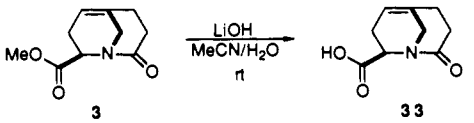

3 **33**

In contrast to the cycloaddition of **22a**, cycloaddition of acetoxy amides **22b** and **22c** proceeded smoothly to give cycloadducts **4** and **5** in 81% and 76% yield, respectively.

As the length of the tether joining the diene to the dienophile in the Diels–Alder reaction is increased, the strain present in the resulting cycloadduct is expected to decrease. On the basis of the successful preparation of bridgehead olefin/amides **3–5**, little difficulty was anticipated in the preparation of cycloadduct **6**, provided that the increased tether length did not produce a serious entropic factor which could slow the reaction.[20]

However, thermolysis of acetate **22d** using the conditions which were successful for the lower homologues (0.01 M in xylenes, 200 °C, 1–2 h) produced the Diels–Alder cycloadduct **6** in only 9%

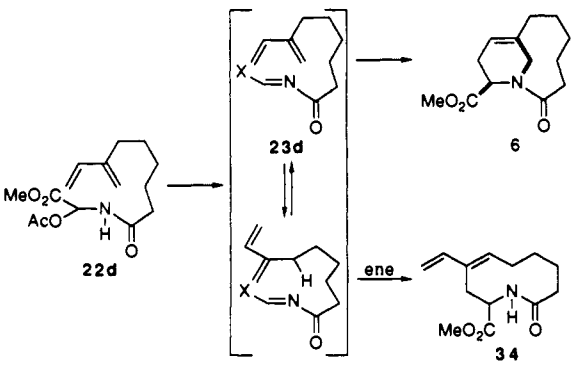

22d **23d** **6** **34**

yield. Among several other products of the thermolysis was a colorless amorphous solid which had a TLC R_f and a GC retention time similar to those of **6**. High-resolution MS of the byproduct showed it had the same molecular weight as the cycloadduct, indicating it was likely formed by some rearrangement of the *N*-acyl imine intermediate. Its room temperature ^{1}H NMR spectrum exhibited only broad, unresolved signals. However, the NMR spectrum became sharper as the ($CDCl_3$) sample was cooled, until at −25 °C a single set of well-resolved peaks was observed. The ^{1}H NMR spectrum of the byproduct also was resolved when the (DMSO-d_6) sample was heated, until at 150 °C a single set of peaks was again observed. This and other (vide infra) spectral data indicate *N*-acyl imine **23d** undergoes an intramolecular ene reaction to give macrocyclic lactam **34**. Lactam **34** was isolated in 25% yield.

The cis configuration of the ring olefin of **34** was determined by difference NOE experiments at −25 °C in $CDCl_3$. The positive enhancements depicted are consistent with cis olefin **34** while the absence of several enhancements indicated in **35** argues against the *trans*-olefin structure. The DNOE analysis assumes a planar s-trans conformation of the 1,3-butadiene moiety.

The ene rearrangement of **22d** to give **34** represents an unprecedented reaction: it is the first example of a type 3 intra-

Scheme II

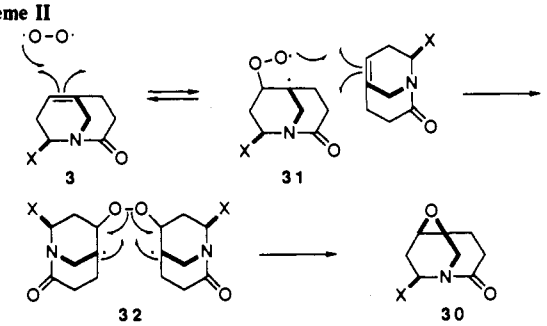

3 **31** **32** **30**

(19) Electrophilic additions to bridgehead olefins: (a) Chiang, Y.; Kresge, A. J.; Wiseman, J. R. *J. Am. Chem. Soc.* **1976**, *98*, 1564. (b) England, W. P. Ph.D. Dissertation, University of California, Irvine, 1988. (c) Shea, K. J.; Kim, J. S. *J. Am. Chem. Soc.* **1992**, *114*, 3044, 4846. Nucleophilic additions to bridgehead lactams: see ref 36.

(20) Shea, K. J.; Burke, L. D.; England, W. P. *J. Am. Chem. Soc.* **1988**, *110*, 860.

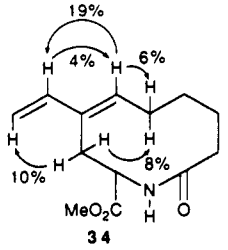

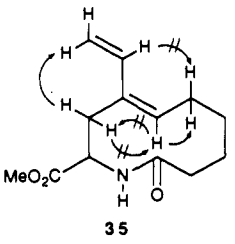

molecular imino ene rearrangement. The term "type 3" indicates that the enophile is tethered to the 3 position of the ene.[21]

Characterization of Cycloadducts. 1. X-ray Crystallography. A. Bridgehead Olefins. X-ray crystallographic studies of bridgehead olefins have revealed two distinct deviations from the optimal planar olefin geometry.[1e] The first is a twisting of the carbon atoms along the C=C internuclear axis such that the p-orbitals are no longer aligned. The second distortion is a rehybridization of the p-orbitals to include some s-character. A complete description of a distorted double bond therefore involves quantifying both the magnitude of the torsional distortion and the degree of rehybridization (pyramidalization) at each of the carbons.

The method used to measure the two independent distortions observed in unsymmetrically deformed double bonds is illustrated in Figure 2.[22] The view along the C_1–C_2 axis of double bond **36** is represented by **37**. Rotation of C_1 relative to C_2 produces a misalignment of the π bond p-orbitals (**38**). The torsional deformation is quantified by the angle τ between the axes of the two p-orbitals. The torsion angle τ is not directly measurable by X-ray crystallography. But, since the p-orbitals are expected to remain orthogonal to the substituents of C_1 and C_2, τ may be determined by measuring either of the four atom torsion angles YC_1C_2W (Φ_1) or ZC_1C_2X (Φ_2). The p-orbital alignment is presumed to be optimal for a double bond in which $\tau = 0.0°$; the poorest overlap should result when $\tau = 90.0°$. Calculations indicate that a double bond in which $\tau = 90°$ corresponds to the first electronically excited state.[23]

The two atoms of the double bond rehybridize independently. For example, consider C_1 of double bond **36** in its undistorted planar geometry (**39**). Incorporation of some s-character into the π bond orbital (rehybridization) produces a pyramidalized atom **40**. The degree of rehybridization of each atom is quantified by the pyramidalization angle χ, defined as the acute angle formed by the projection of one substituent (Z) across the atom onto the geminal substituent (Y). For an $sp^{2.00}$ atom, $\chi = 0.0°$, while, for an $sp^{3.00}$ atom, $\chi = 60.0°$.

In practice, both the torsional and pyramidalization distortions are observed (**41**). The pyramidalization angles χ_1 at C_1 and χ_2 at C_2 are measured as described above. However in the composite structure **41**, Φ_1 and Φ_2 are no longer equivalent and neither is equal to τ. Instead the torsional distortion is defined by the equation $\tau = \Phi_{avg} = (\Phi_1 + \Phi_2)/2$.

In the discussion of the distortions of bridgehead olefins **3–5**, the designations χ_B and χ_E refer to the pyramidalization angles at the bridgehead and exocyclic (to the n+3-membered ring) atoms of the olefin, respectively, as indicated in **42**. The X-ray crystallographic data for cycloadducts **3**, **4**, and **5** provides a complete and detailed description of the distortions of the bridgehead double

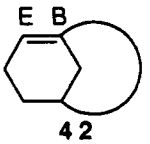

bonds. The X-ray structures are especially valuable because there are little data concerning series of homologous bridgehead olefins in which the size of one bridge is systematically varied.[24] In addition, although several bicyclo[3.3.1]nonene derivatives have been synthesized, none had ever been characterized by X-ray crystallography. The X-ray crystal structure of **3** is the first of any anti-Bredt olefins containing a *trans*-cyclooctene ring. The values and estimated standard deviations of the distortion parameters χ_B, χ_E, and τ for bridgehead olefins **3–5** are presented in Table II.[25]

The bridgehead olefinic carbon atom shows a smooth and significant trend of increased pyramidalization (χ_B) as the *trans*-cycloalkene ring becomes smaller in the homologous series: the χ_B values correspond to hybridization values of $sp^{2.14}$ for **5**, $sp^{2.38}$ for **4**, and $sp^{2.65}$ for **3**. The olefinic bridgehead carbon atoms in **4** and **5** are each significantly pyramidalized but are closer to sp^2 than to sp^3 geometry. Bicyclo[3.3.1]nonene derivative **3**, however, represents the crossover point wherein the topology of the molecule forces the bridgehead carbon atom to adopt a geometry which is closer to sp^3 than to sp^2 hybridization. Pyramidalization at the exocyclic olefinic carbon atom (χ_E) also increases as the *trans*-cycloalkene ring size decreases. (The value of χ_B is always larger than χ_E in a given bridgehead olefin.[1e]) The pyramidalization values correspond to hybridizations of $sp^{2.00}$ for **5**, $sp^{2.14}$ for **4**, and $sp^{2.30}$ for **3**. Thus for all three bridgehead olefins, the exocyclic carbon is closer to sp^2 than to sp^3 geometry.

The p-orbital torsion angle also increases as the size of the *trans*-cycloalkene ring is reduced, although the increase is slightly attenuated in the series. The p-orbital overlap in the π bond should be optimal for $\tau = 0°$ and worst at $\tau = 90°$ (vide supra); therefore, bridgehead olefins **5**, **4**, and **3** suffer 0%, 7%, and 12%, respectively, of the maximum possible p-orbital torsional distortion.

The progression of distortions of the bridgehead olefins in the series **5**, **4**, and **3** is vividly displayed in ORTEP plots of the appropriate portions of the molecules (Figure 3).

The bridgehead olefin and bridgehead lactam functionalities in **3** each reverse the normal preference for the chair–chair conformation in bicyclo[3.3.1]nonane derivatives. Molecular mechanics calculations indicate that chair–chair conformer **43** is 1.4–3.8 kcal/mol more stable than the chair–boat conformer **44**, which is 2.6–5.5 kcal/mol more stable than the boat–boat conformer **45**.[26] Bridgehead olefin **3** is the first boat–boat bicyclo[3.3.1]nonane system (Figure 4).

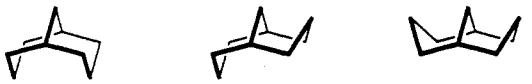

The distortion of the bridgehead double bonds in compounds **3–5** may be compared with those of other [n.3.1] bridgehead

(21) Type I intramolecular imino ene rearrangement: Liu, J.-M.; Koch, K.; Fowler, F. W. *J. Org. Chem.* **1986**, *51*, 167–174. Koch, K.; Liu, J.-M.; Fowler, F. W. *Tetrahedron Lett.* **1983**, 1581–1584.

(22) Winkler, F. K.; Dunitz, J. D. *J. Mol. Biol.* **1971**, *59*, 169–182.

(23) Saltiel, J.; Charlton, J. L. In *Rearrangements in Ground and Excited States*; Mayo, P. d., Ed.; Academic: New York, 1980; Vol. 3, Chapter 7. Michl, J.; Bonacic-Koutecky, V. *Electronic Aspects of Organic Photochemistry*; John Wiley and Sons: New York, 1990.

(24) Shea, K. J.; Cooper, D. C.; England, W. P.; Ziller, J. W.; Lease, T. G. *Tetrahedron Lett.* **1990**, *31*, 6843.

(25) Pyramidalization and torsion angles and their esd's were calculated with use of the OR FFE program: Busing, W. R.; Martin, K. O.; Levy, H. A. *OR FFE: A Fortran Crystallographic Function and Error Program*; Oak Ridge National Laboratory, U. S. Atomic Energy Commision: Oak Ridge, TN, 1964; ORNL-TM-306.

(26) Mastryukov, V. S.; Popik, M. V.; Dorofeeva, O. V.; Golubinskii, A. V.; Vilkov, L. V.; Belikova, N. A.; Allinger, N. L. *J. Am. Chem. Soc.* **1981**, *103*, 1333–1337. Bovill, M. J.; Cox, P. J.; Flitman, H. P.; Guy, M. H. P.; Hardy, A. D. U.; McCabe, P. H.; Macdonald, M. A.; Sim, G. A.; White, D. N. J. *Acta Crystallogr.* **1979**, *B35*, 669–675. Osawa, E.; Aigami, K.; Inamoto, Y. *J. Chem. Soc., Perkin Trans. 2* **1979**, 172–180. Mikhailov, V. K.; Aredova, E. N.; Sevost'yanova, V. V.; Shlyapochnikov, V. A. *Izv. Akad. Nauk SSSR, Ser. Khim. (Engl. Transl.)* **1978**, *27*, 2184–2188. Allinger, N. L.; Tribble, M. T.; Miller, M. A.; Wertz, D. H. *J. Am. Chem. Soc.* **1971**, *93*, 1637–1648. Engler, E. M.; Andose, J. D.; Schleyer, P. v. R. *J. Am. Chem. Soc.* **1973**, *95*, 8005–8025.

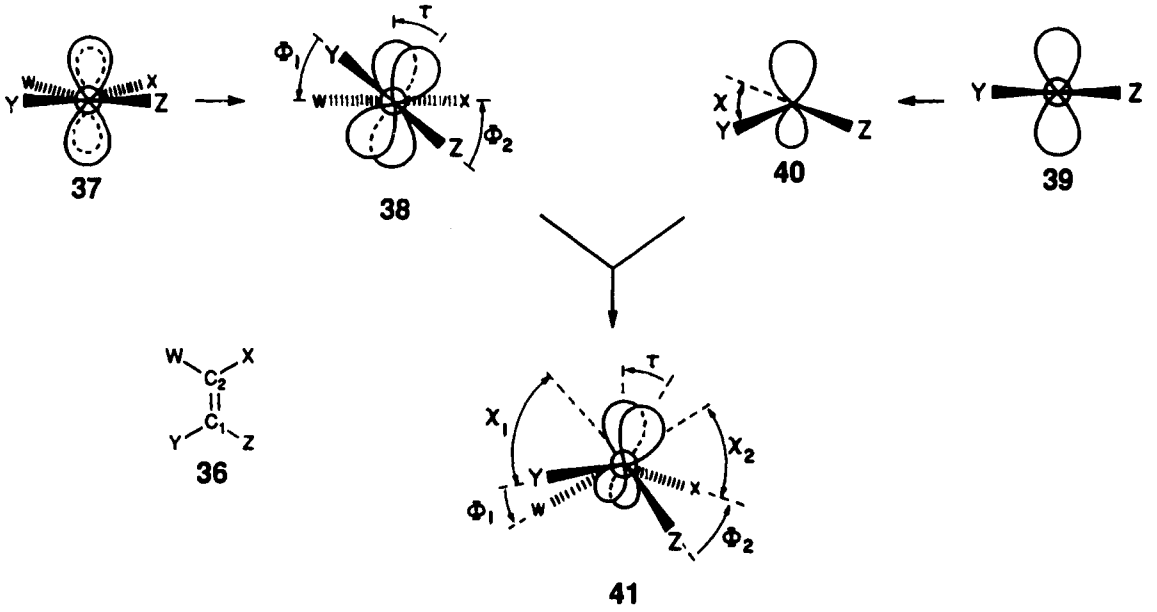

Figure 2. Definitions of distortional parameters χ and τ.

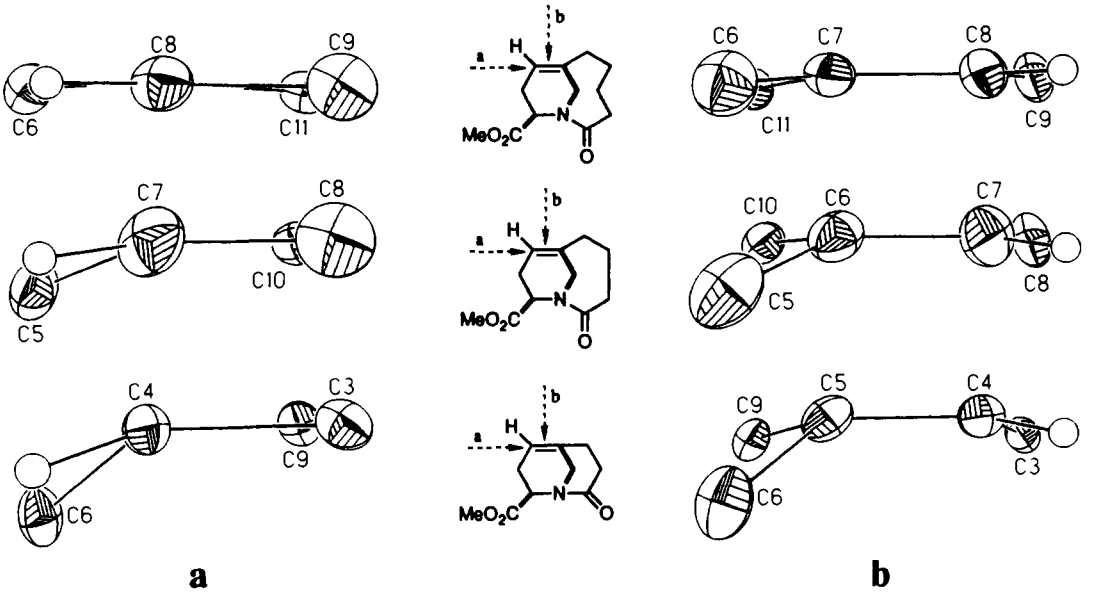

Figure 3. ORTEP plots (at 20% probability level for clarity) of the bridgehead olefin bonds and substituents for **5**, **4**, and **3** with all other atoms omitted: (a) olefins viewed along the axis of the C=C bond with the exocyclic alkene carbon in front (indicated by dashed arrows a); (b) side views (indicated by dashed arrows b).

Table II. Comparison of Distortions in Bridgehead Olefins **3–5** with Those of Other Bridgehead Olefins

bridgehead olefin	χ_B (deg)	χ_E (deg)	τ (deg)	C=C BL (Å)
3	39.0(2)	17.9(1.1)	10.8(5)	1.333(2)
4	22.7(3)	8.2(1.8)	6.4(7)	1.322(4)
5	8.4(3)	0.0(1.3)	0.4(5)	1.328(3)
46	10.9	9.0	4.9	
47	13.1	5.2	9.2	
48	18.7	10.0	6.8	
49	15.0	7.3	3.9	
50	24.3	20.4	19.6	
51	50.3			

olefins for which X-ray crystal structures have been obtained (Table II): cycloadduct **5** may be compared with **46**[27] and **47**,[28] which are representative of fifteen structurally characterized

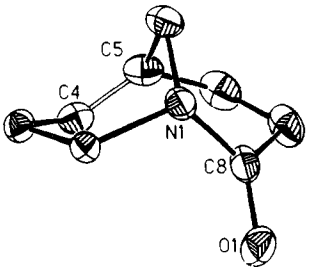

Figure 4. ORTEP plot of bicyclo[3.3.1]nonene derivative **4** indicating the boat-boat conformation.

[5.3.1] bridgehead olefins, and **4** may be compared with two other bicyclo[4.3.1]decene derivatives, **48**[19b] and **49**.[29] The distortions of bridgehead olefin **5** are uniformly smaller than those found in **46** and **47**; indeed, **5** is one of the least distorted among the structurally characterized [5.3.1] bridgehead olefins. In contrast,

(27) Cooper, D. K. Ph.D. Dissertation, University of California, Irvine, 1987.

(28) Haffner, C. D. Ph.D. Dissertation, University of California, Irvine, 1988.

(29) Shea, K. J.; Fruscella, W. M.; Carr, R. C.; Burke, L. D.; Cooper, D. K. *J. Am. Chem. Soc.* **1987**, *109*, 447–452.

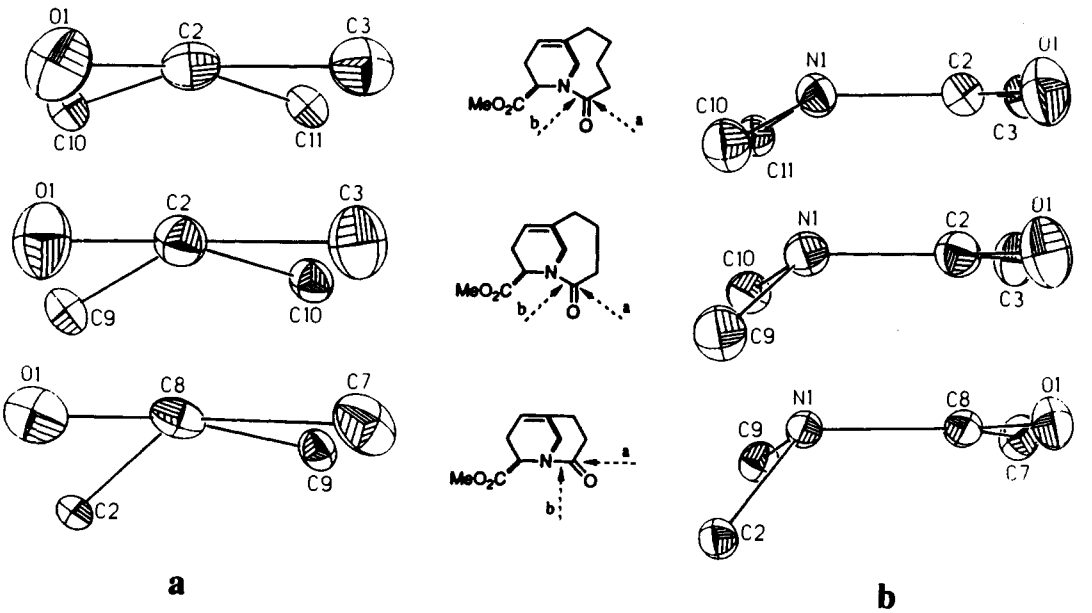

Figure 5. ORTEP plots (at 20% probability level for clarity) of the bridgehead lactam bonds and substituents for **3–5** with all other atoms omitted: (a) lactams viewed along the axis of the C–N bond with the carbonyl carbon in front (indicated by dashed arrows a); (b) side views (indicated by dashed arrows b).

the distortions of **4** do not appear abnormal compared to those of bridgehead olefins of the same ring size.

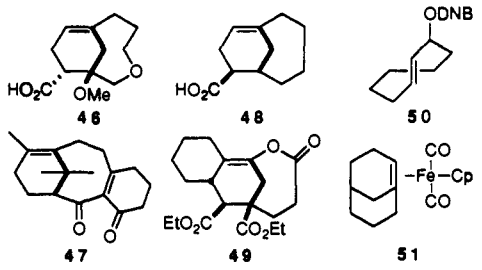

Since **3** is the only bicyclo[3.3.1]nonene derivative which has been structurally characterized, it is impossible to compare its distortions with those of other bridgehead olefins of the same ring size. However, **3** may be compared with *trans*-cyclooctene derivative **50**[30] and transition metal-bound bicyclo[3.3.1]nonene **51**.[31] A neutron diffraction study of **50** indicated pyramidalization values χ comparable to the χ_E value but approximately half as large as the χ_B observed in **3** and a p-orbital torsion value nearly twice as large as that observed in **3**. An X-ray diffraction study of **50** gave results similar to those of the neutron diffraction study. The large χ_B value found in **51** may be attributed to the metallacyclopropane character of the iron–olefin complex. The χ_E and τ parameters cannot be determined because the hydrogen atom positions were not reported for **51**.

The strain present in a bridgehead olefin is expected to be manifest in a weaker C=C bond which, in turn, may be expected to correlate with an increased bond length. However, no trend is observed in the C=C bond lengths of bridgehead olefins **3–5** (Table II). The observed values are close to the C=C bond length in cyclohexene (1.335(3) Å)[32] and are far from the bond length of 1.543 Å for the C—C single bond at the same (boat cyclohexane) position in bicyclo[3.3.1]nonane derivative **52**.[33] Thus,

Table III. Distortion Parameters and Bond Lengths of Bridgehead Lactams **3–5**

lactam	χ_N (deg)	χ_C (deg)	τ (deg)	C=O BL (Å)	C—N BL (Å)
3	54.9(1)	1.4(2)	16.7(1)	1.215(2)	1.399(2)
4	46.4(2)	1.2(3)	7.5(2)	1.219(2)	1.375(2)
5	38.2(2)	−0.2(3)	0.9(2)	1.224(2)	1.376(2)

the bond lengths of the bridgehead olefins are insensitive functions of the geometric distortions.

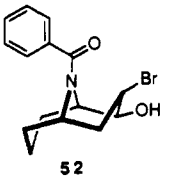

52

B. Bridgehead Lactams. Table III contains the distortion parameters and bond lengths for bridgehead lactams **3–5**. The pyramidalization angles at nitrogen, χ_N, and at the carbonyl carbon, χ_C, are analogous to the pyramidalization angles χ_B and χ_E at the bridgehead and exocyclic carbon atoms, respectively, of bridgehead olefins. The p-orbital torsion angle τ represents the angle between the axis of the nitrogen lone-pair orbital and that of the carbonyl carbon p-orbital.

Pyramidalization of the lactam nitrogen atom is significant in each of the cycloadducts. Further, there is a noticeable and smooth increase in the distortion as the trans lactam ring size is decreased. The χ_N values correspond to hybridization values of $sp^{2.64}$ for **5**, $sp^{2.77}$ for **4**, and $sp^{2.92}$ for **3**. Thus, the topologic constraints of the bicyclic systems produce an "amide" nitrogen atom which is more nearly sp^3 than sp^2 even for the [5.3.1] cycloadduct **5**; and the rehybridization to sp^3 geometry is nearly complete for the [3.3.1] cycloadduct **3**.

Pyramidalization of the lactam carbonyl carbon, however, is not significant in any of the three bridgehead lactams. The atom remains essentially planar throughout the homologous series: it is $sp^{2.00}$ hybridized in **5** and $sp^{2.02}$ hybridized in **3** and **4**. The p-orbital torsion angle τ increases steadily in the series: bridgehead lactams **5**, **4**, and **3** suffer 1%, 8%, and 19%, respectively, of the maximum p-orbital torsional distortion.

The progression of distortions of the bridgehead lactams in the series **3–5** is readily discerned from ORTEP plots of the appro-

(30) Ermer, O.; Mason, S. A. *Acta Crystallogr.* **1982**, *B38*, 2200–2206.

(31) Bly, R. S.; Hossain, M. M.; Lebioda, L. *J. Am. Chem. Soc.* **1985**, *107*, 5549–5550.

(32) Determined by electron diffraction: Chiang, J. F.; Bauer, S. H. *J. Am. Chem. Soc.* **1969**, *91*, 1898–1901.

(33) Determined by X-ray crystallography: Tamura, C.; Sim, G. A. *J. Chem. Soc. B* **1968**, 1241–1248.

Table IV. Comparison of the Distortions of the Olefin and Lactam in **3–5**

	3	4	5
olefin χ_B	39.0	22.7	8.4
lactam χ_B (X_N)	54.9	46.4	38.2
$\Delta\chi_B$	15.9	23.7	29.8
olefin χ_E	17.9	8.2	0.0
lactam χ_E (χ_C)	1.4	1.2	−0.2
$\Delta\chi_B$	−16.5	−7.0	0.2
olefin τ	10.8	6.4	0.4
lactam τ	16.7	7.5	0.9
$\Delta\tau$	5.9	1.1	0.5

priate portions of the molecules (Figure 5).

Comparison of the pyramidalization and torsional distortions of the bridgehead lactams to those of the bridgehead olefins reveals the lactam functionality is more easily distorted than the olefin. This may be understood by considering the alternative resonance forms of the bridgehead double bond for each case. The bridgehead lactam has two energetically important resonance contributors: both the zwitterionic (bridgehead double bond) form **53** and the amino ketone form **54** possess closed-shell octets for

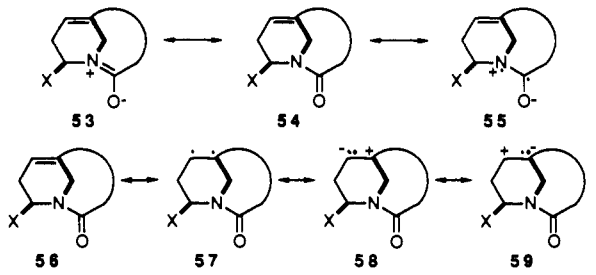

53 **54** **55**

56 **57** **58** **59**

the relevant atoms. Resonance forms such as **55** are expected to make minor contributions. However, for the bridgehead olefin, the only resonance forms of the bridgehead double bond in **56** are the diradical **57** or zwitterions **58** and **59**. Resonance forms **57–59** represent high-energy species and, therefore, do not make an important contribution to the electronic structure of the olefin. Thus, the bridgehead lactams are more easily distorted, since they have an energetically accesible resonance form in which the lactam is distorted from planarity; but distortion of the olefins is more difficult, since only the double-bond resonance form is energetically accessible.

Table IV compares the χ and τ values of the bridgehead lactam and bridgehead olefin for cycloadducts **3–5**. Pyramidalization at the bridgehead position is greater in each case for the lactam than for the olefin, indicating the important resonance contribution of amino ketone resonance form **54**, in which the nitrogen atom is tetrahedral. The decreasing value of $\Delta\chi_B$ in the series **3–5** indicates the difference in the bending potentials of the bridgehead atoms of the two functional groups.

The increasing value of the bridgehead olefins' χ_E compared to the near monotonic value of the bridgehead lactams' χ_C is a further indication of the contribution of amino ketone resonance form **54** to the electronic structure of the bridgehead lactam. Pyramidalization of the exocyclic carbon of the bridgehead olefin decreases the value of τ.[1e] But the ketone functionality is stable regardless of the lactam τ value. Thus while an increase in the bridgehead olefin χ_E value in the series **3–5** is necessary in order to obtain the energetic minimum, the bridgehead lactam χ_C value remains near zero because overlap of the carbonyl π bond with the nitrogen lone pair is not essential to the molecules' stability. Although the increase in the τ value of the bridgehead olefins is attenuated in the series **3–5**, the increase in the τ value of the bridgehead lactams is slightly accelerated.

The classic view of amidic resonance predicts that the C=O bond should be longer in amides than in ketones and that the amide C—N bond should be shorter than a C—N bond in which the nitrogen lone pair is not conjugated with a carbonyl π system. The X-ray crystallographic data for homologous bridgehead lactams **3–5**, therefore, provide the opportunity to quantify the loss of amidic resonance in terms of the C=O and C—N bond lengths. Table III lists the appropriate internuclear distances for the bridgehead lactams **3–5**.

The C=O bond of homologous bridgehead lactams **3–5** becomes progressively shorter as the distortions increase. The trend indicates amino ketone resonance form **54**, which contains the carbon–oxygen double bond, is becoming relatively more important than zwitterionic resonance form **53**, which contains the carbon–oxygen single bond, as the distortions of the amide are increased. Further, the C=O bond length in all three of the cycloadducts is much closer to the bond length found in cyclohexanone (1.222 Å)[34] than to that found in valerolactam (1.243(2) Å);[35] in fact bridgehead lactams **3** and **4** each possess an amide C=O bond shorter than the cyclohexanone carbonyl bond. Thus, the amide carbonyl bond length in cycloadducts **3–5** is more like that of a ketone than that of a normal lactam.

The C–N bond lengths of **4** and **5** are within error of one another; but that of **3** is significantly longer. Although the trend is not smooth, the amino ketone resonance form **54** (C—N bond) appears to become relatively more important than the zwitterionic amide resonance form **53** (C=N bond) as the distortions of the bridgehead lactam increase. The C—N bond length in **5** and **4** is significantly longer than that found in valerolactam (1.333(2) Å) but is closer to this value than to the bond length in piperidine[36] (1.472(11) Å). However, the bond distance in lactam **3** is halfway between those of the normal amide C—N bond and the single C—N bond. Thus, in contrast to the bridgehead olefin bond distances, the bridgehead lactam bond lengths are sensitive functions of the geometric distortions.

While the C—N bond in bridgehead lactam **3** is 0.024 Å longer than those in **4** and **5**, the C=O bond is only 0.009 Å shorter than that in **5**. This phenomenon has also been observed in a computational investigation of the origin of the rotational barrier in amides.[37] Instead of the classical charge-transfer resonance picture, Wiberg proposed that the barrier to rotation in amides arises from natural electronic tendencies. Some experimental support for this hypothesis has been provided: Brown[38] has attempted to develop a model for enzyme-mediated amide hydrolysis and has investigated the hydrolysis rates of the structurally distorted lactams **60a–d**. In fact the rate of hydrolysis of **60a–d** could be correlated to χ_N but not to τ.

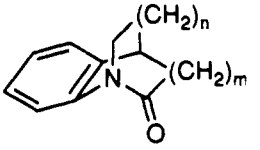

60a: m=n=2
60b: m=2, n=1
60c: m=1, n=2
60d: m=n=1

The reactivities of lactams **3–6** are currently being examined in order to determine the deformation modes that activate the amide linkage toward hydrolysis.

C. Comparison of X-ray Data to MM2 Calculations. The X-ray crystal structure data collected for cycloadducts **3–5** allows a comparison of the olefin and amide geometries determined ex-

(34) Determined by microwave spectroscopy: Ohnishi, Y.; Kozima, K. *Bull. Chem. Soc. Jpn.* **1968**, *41*, 1323.

(35) Helm, D. v. d.; Ekstrand, J. D. *Acta Crystallogr.* **1979**, *B35*, 3101–3103.

(36) Gundersen, G.; Rankin, D. W. H. *Acta Chem. Scand., Ser. A* **1983**, *A37*, 865–874.

(37) Wiberg, K. B.; Laidig, K. E. *J. Am. Chem. Soc.* **1987**, *109*, 5935–5943.

(38) Wang, Q.-P.; Bennett, A. J.; Brown, R. S.; Santarsiero, B. D. *J. Am. Chem. Soc.* **1991**, *113*, 5757–5765. Skorey, K. I.; Somayaji, V.; Brown, R. S. *J. Am. Chem. Soc.* **1989**, *111*, 1445–1452. Somayaji, V.; Keillor, J.; Brown, R. S. *J. Am. Chem. Soc.* **1988**, *110*, 2625–2629. Skorey, K. I.; Somayaji, V.; Brown, R. S. *J. Am. Chem. Soc.* **1988**, *110*, 5205–5206. Somayaji, V.; Brown, R. S. *J. Am. Chem. Soc.* **1987**, *109*, 4738–4739. Slebocka-Tilk, H.; Brown, R. S. *J. Org. Chem.* **1987**, *52*, 805–808. Somayaji, V.; Brown, R. S. *J. Org. Chem.* **1986**, *51*, 2676–2686.

Table V. Comparison of MM2 and X-ray Geometries of Bridgehead Olefins

compound	χ_B	χ_E	τ	bond length (Å)
$3_{X\text{-}ray}$	39.0(2)	17.9(1.1)	10.8(5)	1.333(2)
3_{MM2}	38.7	21.4	12.3	1.349
$4_{X\text{-}ray}$	22.7(3)	8.2(1.8)	6.4(7)	1.323(4)
4_{MM2}	23.5	11.1	6.6	1.346
$5_{X\text{-}ray}$	8.4(3)	0.0(1.3)	0.4(5)	1.328(3)
5_{MM2}	6.3	0.9	2.0	1.345

perimentally with those calculated by molecular mechanics programs. The lowest energy conformation of compounds **3–5** was calculated using the MM2 force field[39] employed in the Macromodel[40] molecular mechanics program. The calculated bridgehead olefin pyramidalization angles χ, torsion angles τ, and C=C bond lengths are compared to the X-ray data in Table V.

MM2 provided good approximations of the pyramidalization at the bridgehead atom, χ_B, of the anti-Bredt olefins; however, the external pyramidalization angle, χ_E, was slightly overestimated. The MM2 force field also overestimated the π twist angle τ by a small amount. The C=C bond lengths calculated were approximately 0.02 Å longer than those found by X-ray crystallography. In general, the MM2 program approximated the geometry of the bridgehead olefins extremely well, including the large deviations from planarity observed for the highly distorted olefin in **3**.

The MM2-calculated geometries of the bridgehead lactam functionalities were also examined (Table VI). MM2 was not as successful in predicting the geometry of the bridgehead amides as it was for the bridgehead olefins. The pyramidalization angle at nitrogen, χ_N, was significantly underestimated by MM2. The pyramidalization angle at the carbonyl, χ_C, was predicted to within 2°. The MM2-calculated π twist angle τ was greater than those observed by X-ray crystallography, the difference being most significant when the observed τ was small.

The error in the calculated C=O bond length does not appear to be systematic; however, the calculated C—N bond length was significantly greater than the observed length when the actual distortions of the bridgehead lactam were relatively small.

2. IR Spectroscopy. Bridgehead Lactams. The infrared C=O stretching absorbance of amides occurs at lower frequencies than that of "normal" carbonyl compounds.[41] This effect is attributed to the partial single-bond character of the C=O bond arising from the zwitterionic amide resonance form. IR spectroscopy may therefore be used to detect loss of this resonance in, and thereby quantify the distortions of, the bridgehead lactams by observing the C=O stretching frequency.

The amide C=O stretching frequency of bridgehead amides **3–6** increases as the size of the *trans*-lactam ring decreases. The observed frequencies for the Diels–Alder cycloadducts are 1641 cm^{-1} (NaCl film) for **6**; 1645 cm^{-1} (KBr) for **5**; 1660 cm^{-1} (KBr) for **4**; and 1703 cm^{-1} (C_6D_6) for **3**. The absorbances for cycloadducts **5** and **6** are near the value expected for a lactam with six or more atoms in the ring. The steady increase in the observed amide carbonyl stretching frequency is interpreted as an indication of the loss of amidic resonance as the amide functionality becomes more distorted. In this regard it is significant that [5.3.1] cycloadduct **5** displays its band at 1645 cm^{-1}, at or below the value expected: although **5** has a p-orbital torsion angle τ of only 0.9°, the amide nitrogen is significantly pyramidalized. Thus by the IR criterion, effective amidic resonance is obtained by the interaction of a planar carbonyl group with a significantly pyramidalized nitrogen atom. The apparent diminution of amidic resonance in **3** and **4** is not easily attributed to a single distortion, since both χ_N and τ increase steadily in the series **5–4–3**.

(39) Bukert, U.; Allinger, N. L. *Molecular Mechanics*; American Chemical Society: Washington, DC, 1982.
(40) Still, W. C. Macromodel, Version 3.0. Columbia University, 1986.
(41) Silverstein, R. M.; Bassler, G. C.; Morrill, T. C. *Spectrometric Identification of Organic Compounds*; John Wiley and Sons: New York, 1981; p 125.

Table VI. Comparison of MM2 and X-ray Geometries of Bridgehead Lactams

lactam	χ_N (deg)	χ_C (deg)	τ (deg)	C=O BL (Å)	C—N BL (Å)
$3_{X\text{-}ray}$	54.9(1)	1.4(2)	16.7(1)	1.215(2)	1.399(2)
3_{MM2}	39.0	3.5	21.9	1.218	1.406
$4_{X\text{-}ray}$	46.4(2)	1.2(3)	7.5(2)	1.219(2)	1.375(2)
4_{MM2}	28.8	3.0	17.9	1.219	1.400
$5_{X\text{-}ray}$	38.2(2)	−0.2(3)	0.9(2)	1.224(2)	1.376(2)
5_{MM2}	20.1	1.6	11.9	1.220	1.399

Table VII. C=O Stretching Frequencies of Bridgehead Lactams and Corresponding Ketones

lactam	ν_{CO} (cm^{-1})	ketone	ν_{CO} (cm^{-1})	$\Delta\nu_{CO}$
3	1703	**61**	1712	−9
4	1660	**62**	1705	−45
5	1645	**63**	1700	−55
6	1641	**64**	unknown	?

Table VIII. NMR Chemical Shifts (ppm) for Cycloadducts **3–6** in C_6D_6 Solvent

compound	vinyl proton	bridgehead carbon	exocyclic carbon	lactam carbonyl
3	5.071	151.952	123.630	182.64
4	5.022	148.772	118.605	180.58
5	5.101	145.052	122.348	177.35
6	5.131	143.648	123.546	173.71

Comparison of the C=O stretching frequencies observed for cycloadducts **3–5** to those observed for homologous bridgehead olefin ketones **61–63** shows a trend (Table VII). Although ν_{CO}

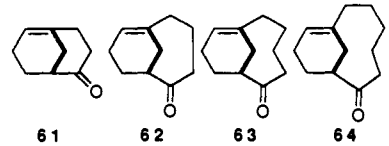

61 **62** **63** **64**

decreases in the series **61**[7a]–**62**–**63**,[42] the amide C=O frequency decreases more rapidly in the series **5–4–3**. (Bridgehead olefin **64** is unknown, so comparison with bridgehead lactam **6** is impossible.) The $\Delta\nu$ values observed for the [5.3.1] and [4.3.1] bicyclic systems indicate the loss of amidic resonance for those bridgehead lactams. The $\Delta\nu$ value of −9 cm^{-1} for the [3.3.1] molecules indicates an even more substantial loss of resonance in **3**.

3. NMR Spectroscopy. A. Bridgehead Olefins. The strain of cycloadducts **3–6** is expected to be manifest in electronic changes of the bridgehead olefin and amide. NMR spectroscopy may therefore be used to detect the variation in strain as a function of ^1H and ^{13}C chemical shift.

As the size of the *trans*-cycloalkene ring in **3–6** is reduced, the attendant distortion of the C=C bond is expected to make overlap of the p-orbitals less effective. This reduced overlap may make one or more alternative resonance forms of the olefin important. The C=C bond in **56** may be heterolytically polarized as that in **58** or **59**; or diradical resonance form **57** may become important. The ^1H NMR chemical shift of the vinyl proton and ^{13}C NMR chemical shifts of the bridgehead and exocyclic olefin carbons in **3–6** are presented in Table VIII.

The chemical shift data for bridgehead olefins **3–6** are most consistent with an increasing contribution of zwitterionic resonance form **58** to the electronic structure of the bridgehead olefin. The steady increase in chemical shift for the bridgehead carbon as the *trans*-cycloalkene ring size decreases is indicative of increasing cationic character. The decreasing chemical shifts of the vinyl proton and exocyclic carbon in bridgehead olefins **6–4** are also consistent with increasing carbanionic character at the exocyclic position. The downfield shifts observed for both the vinyl proton

(42) Gilman, J. W. Ph.D. Dissertation, University of California, Irvine, 1985.

and exocyclic carbon in **3**, however, are not in agreement with this model. This effect may be due to deshielding of the exocyclic carbon position by the amide π system: examination of molecular models reveals the bridgehead lactam may be suitably positioned to induce such an effect in **3**, but is not similarly oriented in **4–6**.

B. Bridgehead Lactams. NMR spectroscopy also provides a means of quantifying the amide vs amino ketone character of the bridged bicyclic lactams by observing the lactam carbonyl ^{13}C chemical shifts (Table VIII). The ^{13}C chemical shift decreases by approximately 9 ppm in the series **3–6**. The smooth trend toward lower field absorbance is evidence that the carbonyl group is becoming more ketonic and less amidic as the strain of the bridgehead olefin increases.

The chemical shift values of bridgehead lactams **3–6** are closer to that observed for *N*-methylvalerolactam (169 ppm) than to that for 2-methylcyclohexanone (210.3 ppm).[3b] Thus the ^{13}C NMR absorbance of [6.3.1] lactam **6** is only 5 ppm greater than that of the reference lactam, but 38 ppm lower than that of the reference ketone. Even the most strained cycloadduct, **3**, displays a chemical shift which is 14 ppm greater than that of the reference lactam but 29 ppm lower than that of the reference ketone. By this measure, bridgehead lactams **3–6** seem to more closely resemble amides than amino ketones.

Conclusion

The structural distortions of a homologous series of bridgehead olefin/bridgehead lactams has been documented. The study has permitted comparison of the response to torsional distortions of the carbon–carbon double bond to the quasi double bond of the amide linkage. It has been possible to qualitatively evaluate the structural requirements for amidic resonance from an analysis of both structural and spectroscopic data. The fact that the "soft" nitrogen bending potential of the amidic nitrogen occurs without significant loss of resonance is the most conspicuous difference between the two linkages. The homologous series of compounds will form the basis of quantitative studies to evaluate the kinetic reactivity of bridgehead amides and olefins.

Experimental Section

General Procedures. Proton nuclear magnetic resonance spectra (^1H NMR) were determined using General Electric QE-300 (300-MHz) or General Electric GN-500 (500-MHz) spectrometers. Carbon nuclear magnetic resonance spectra (^{13}C NMR) were determined using the above instruments operating at 75.4 MHz (QE-300) or 125.7 MHz (GN-500). Chemical shifts are reported as delta (δ) values relative to internal tetramethylsilane. Coupling constants (J) are reported in Hertz (Hz); abbreviations used are s, singlet; d, doublet; t, triplet; q, quartet; dd, doublet of doublets, etc.; m, multiplet; br, broad. Infrared spectra were recorded with an Analect RFX-40 FTIR spectrometer. High-resolution mass spectra (EI, 20 eV) were recorded on a VG Analytical 7070E high-resolution mass spectrometer. Gas chromatographic analyses were carried out using a Hewlett-Packard 5790 chromatograph and 3390A recorder–integrator or a Hewlett-Packard 5890 chromatograph and 3396A recorder–integrator. Each chromatograph was equipped with a 0.2 mm diameter methyl silicone capillary column and fitted with a flame ionization detector.

Most reagent grade chemicals and solvents were purified and dried by standard methods.[43] Tetrahydrofuran and diethyl ether were distilled from potassium metal and benzophenone; pyridine, triethylamine, benzene, toluene, xylenes, acetonitrile, hexane, and methylene chloride were distilled from CaH_2 under N_2. Chromatography refers to either liquid flash-column chromatography[44] or liquid radial chromatography. Radial chromatography was done with a Harrison Research Chromatotron. TLC, column, and radial chromatography were done with E. Merck silica gel. Hexane and ethyl acetate used in chromatography were distilled. All reactions were run under an N_2 atmosphere; concentrations were done under reduced pressure with use of a Büchi rotary evaporator.

6-(Tetrahydropyranyloxy)hexan-1-ol (15). A solution of 1,6-hexanediol (40.9 g, 0.346 mol), dihydropyran (14.6 g, 0.174 mol, 0.50 equiv), and HCl (2 drops) was stirred at room temperature for 3.5 h. The mixture was poured into a solution of water (50 mL) and saturated aqueous NaCl solution (100 mL) and extracted with 3:1 petroleum ether/Et_2O (300 mL + 3 × 100 mL). Chromatography (2:1 hexane/EtOAc, R_f 0.15) followed by distillation (bp 112–114 °C, 0.65 mm) afforded 18.4 g (91.0 mmol, 52%) of a colorless oil. ^1H NMR (500 MHz, $CDCl_3$) δ 4.52 (dd, J = 4.4 Hz, J = 2.7 Hz, OC*H*O), 3.82 (ddd, J = 11.2 Hz, J = 7.6 Hz, J = 3.5 Hz, 1 H), 3.69 (dt, J = 9.6 Hz, J = 6.9 Hz, 1 H), 3.58 (dt, J = 3.4 Hz, J = 6.2 Hz, 2 H), 3.45 (m, 1 H), 3.34 (dt, J = 9.6 Hz, J = 6.6 Hz, 1 H), 1.79 (m, 2 H), 1.66 (m, 1 H), 1.52 (m, 7 H), 1.34 (m, 4 H); ^{13}C NMR (125 MHz, $CDCl_3$) δ 98.86, 67.52, 62.76, 62.39, 32.67, 30.73, 29.66, 25.99, 25.56, 25.46, 19.68; IR (NaCl film) 3408, 2937, 2862, 1352, 1201, 1138, 1120, 1078, 1034, 984 cm^{-1}; MS (CI, isobutane) 203.1649 (203.1647 calcd for $C_{11}H_{22}O_3$ + H).

6-(Tetrahydropyranyloxy)-1-iodohexane (16). A solution of alcohol **15** (18.4 g, 91.0 mmol) and triethylamine (9.8 g, 96.9 mmol, 1.06 equiv) in CH_2Cl_2 (400 mL) cooled to 0 °C was treated with methanesulfonyl chloride (11.1 g, 96.9 mmol, 1.06 equiv). After 1 h the mixture was washed with successive 100-mL portions of cold water, 5% aqueous HCl solution, saturated aqueous $NaHCO_3$ solution and saturated aqueous NaCl solution. The organic phase was dried ($MgSO_4$) and concentrated to give a colorless oil.

A solution of the crude mesylate and sodium iodide (27.3 g, 182 mmol, 2.00 equiv) in acetone (500 mL) was heated to reflux for 11 h. The mixture was filtered, and the insoluble solids were washed with acetone (3 × 50 mL). The filtrate was concentrated and the residue dissolved in Et_2O (150 mL). The organic phase was washed with water (100 mL) and saturated aqueous $Na_2S_2O_3$ solution (100 mL). Chromatography (9:1 hexane/EtOAc, R_f 0.35) afforded 19.4 g (62.1 mmol, 68%) of a colorless oil. ^1H NMR (500 MHz, $CDCl_3$) δ 4.57 (dd, J = 4.4 Hz, J = 2.8 Hz, OC*H*O), 3.86 (ddd, J = 11.1 Hz, J = 7.6 Hz, J = 3.4 Hz, 1 H), 3.73 (dt, J = 9.6 Hz, J = 6.8 Hz, 1 H), 3.50 (m, 1 H), 3.38 (dt, J = 9.6 Hz, J = 6.5 Hz, 1 H), 3.19 (t, J = 7.0 Hz, C*H*$_2$I), 1.84 (m, 3 H), 1.70 (m, 1 H), 1.56 (m, 6 H), 1.40 (m, 4 H); ^{13}C NMR (125 MHz, $CDCl_3$) δ 98.84, 67.36, 62.35, 33.41, 30.71, 30.27, 29.48, 25.42, 25.19, 19.65, 7.11; IR (NaCl film) 2937, 2864, 1201, 1169, 1134, 1119, 1078, 1034, 1022 cm^{-1}; MS (CI, isobutane) 313.0658 (313.0665 calcd for $C_{11}H_{21}IO_2$ + H).

7-Methylenenon-8-enol (18d). A solution of iodide **16** (19.4 g, 62.1 mmol) and lithium chloride/cupric chloride (0.106 M in THF, 1.27 mmol, 0.02 equiv) in THF (150 mL) was treated with a solution of 1,3-butadien-2-ylmagnesium chloride (0.643 M in THF, 68.2 mmol, 1.10 equiv). After 18 h the mixture was poured into saturated aqueous NH_4Cl solution (100 mL) and 5% aqueous HCl solution (25 mL). The mixture was extracted with hexane (2 × 200 mL). The organic phase was washed with saturated aqueous $Na_2S_2O_3$ solution (100 mL) and saturated aqueous NaCl solution (100 mL), dried ($MgSO_4$), and concentrated to give a pale-yellow oil.

A solution of the crude THP-protected diene alcohol **17** and pyridinium *p*-toluenesulfonate (1.55 g) in absolute ethanol (200 mL) was heated to 60 °C for 2 h. The mixture was concentrated to approximately 50 mL and poured into water (200 mL) and saturated aqueous NaCl solution (50 mL). The aqueous phase was extracted with Et_2O (200 mL + 3 × 100 mL). Chromatography (2:1 hexane/EtOAc, R_f 0.36) afforded 5.77 g (37.4 mmol, 60%) of an oil. ^1H NMR (500 MHz, $CDCl_3$) δ 6.36 (dd, J = 17.6 Hz, J = 10.8 Hz, H_2C=C*H*), 5.22 (d, J = 17.6 Hz, *H*HC=CH), 5.05 (d, J = 10.8 Hz, H*H*C=CH), 5.00 (s) and 4.98 (s) (C*H*$_2$=C), 3.64 (t, J = 6.6 Hz, C*H*$_2$OH), 2.21 (t, J = 7.7 Hz, CC*H*$_2$), 1.58 (tt, J = 7.2 Hz, J = 7.2 Hz) and 1.50 (tt, J = 7.1 Hz, J = 7.1 Hz) (CCH$_2$C*H*$_2$ and C*H*$_2$CH$_2$OH), 1.38 (m, C*H*$_2$C*H*$_2$C*H*$_2$C*H*$_2$O*H*); ^{13}C NMR (125 MHz, $CDCl_3$) δ 146.36, 138.91, 115.50, 113.04, 62.96, 32.69, 31.19, 29.29, 28.02, 25.56; IR (NaCl film) 3336, 3089, 2933, 2860, 1595, 1464, 1074, 1057, 1036, 991, 895 cm^{-1}; MS (CI, isobutane) 155.1435 (155.1436 calcd for $C_{10}H_{18}O$ + H).

7-Methylenenon-8-enoic Acid (19d). A solution of alcohol **18d** (1.66 g, 10.8 mmol) in DMF (10 mL) was added dropwise over 30 min to a cooled (0 °C) solution of pyridinium dichromate (15.1 g, 40.2 mmol, 3.72 equiv) in DMF (50 mL). The mixture was allowed to warm to room temperature. After 8 h the mixture was poured into water (350 mL) and extracted with 1:1 petroleum/Et_2O (6 × 100 mL). Chromatography (1:1 hexane/EtOAc, R_f 0.46) afforded 1.24 g (7.37 mmol, 68%) of a colorless oil. ^1H NMR (500 MHz, $CDCl_3$) δ 6.36 (dd, J = 17.6 Hz, J = 10.8 Hz, H_2C=C*H*), 5.21 (d, J = 17.6 Hz, *H*HC=CH), 5.05 (d, J = 10.8 Hz, H*H*C=CH), 5.00 (s) and 4.97 (s) (C*H*$_2$=C), 2.36 (t, J = 7.5 Hz, C*H*$_2$CO), 2.21 (t, J = 7.7 Hz, CC*H*$_2$), 1.66 (tt, J = 7.6 Hz, J = 7.6 Hz) and 1.51 (tt, J = 7.6 Hz, J = 7.6 Hz) (CCH$_2$C*H*$_2$ and C*H*$_2$CH$_2$CO), 1.38 (tt, J = 7.6 Hz, J = 7.6 Hz, C*H*$_2$CH$_2$CH$_2$CO); ^{13}C NMR (125 MHz, $CDCl_3$) δ 179.98, 146.19, 138.89, 115.68, 113.15, 33.98, 31.08, 28.94, 27.70, 24.52; IR (NaCl film) 3089, 3041, 3006, 2937, 2864, 1711, 1595, 1414, 991, 897 cm^{-1}; MS (EI) 168.1154 (168.1150 calcd for $C_{10}H_{16}O_2$).

5-Methylenehept-6-enoic Acid (19b). Prepared 0.73 g (51%) following the above procedure. ^1H NMR (500 MHz, $CDCl_3$) δ 6.34 (dd, J = 17.6

(43) Perrin, D. D.; Armarego, L. F.; Perrin, D. R. *Purification of Laboratory Chemicals*; Pergamon: New York, 1966.
(44) Still, W. C.; Kahn, M. *J. Org. Chem.* **1978**, *43*, 2923.

Hz, J = 10.8 Hz, H_2C=CH), 5.22 (d, J = 17.6 Hz, HHC=CH), 5.05 (d, J = 11.0 Hz, HHC=CH), 5.03 (s) and 4.99 (s) (CH_2=C), 2.38 (t, J = 7.4 Hz) and 2.26 (t, J = 7.8 Hz) ($CH_2CH_2CH_2$), 1.83 (tt, J = 7.5 Hz, J = 7.5 Hz, $CH_2CH_2CH_2$); ^{13}C NMR (125 MHz, $CDCl_3$) δ 180.00, 145.17, 138.48, 116.43, 113.55, 33.55, 30.56, 22.96; IR (NaCl film) 3089, 3039, 3006, 2939, 2671, 1707, 1595, 1414, 1298, 1244, 993, 899 cm^{-1}; MS (CI, isobutane) 141.0885 (141.0915 calcd for $C_8H_{12}O_2$ + H).

6-Methyleneoct-7-enoic Acid (19c). Prepared 0.75 g (56%) following the above procedure. ^{1}H NMR (500 MHz, $CDCl_3$) δ 6.34 (dd, J = 17.6 Hz, J = 10.8 Hz, H_2C=CH), 5.19 (d, J = 17.6 Hz, HHC=CH), 5.04 (d, J = 10.9 Hz, HHC=CH), 5.00 (s) and 4.97 (s) (CH_2=C), 2.36 (t, J = 7.4 Hz) and 2.21 (dt, J = 1.0 Hz, J = 7.6 Hz) (CCH_2 and CH_2CO), 1.66 (tt, J = 7.6 Hz, J = 7.6 Hz) and 1.53 (m) ($CH_2CH_2CH_2CH_2$); ^{13}C NMR (125 MHz, $CDCl_3$) δ 180.03, 145.77, 138.79, 115.90, 113.23, 33.92, 30.91, 27.44, 24.53; IR (NaCl film) 3089, 3039, 3006, 2937, 2866, 1709, 1595, 1414, 1284, 1236, 899 cm^{-1}; MS (EI) 154.1001 (154.0994 calcd for $C_9H_{14}O_2$).

7-Methylenenon-8-enamide (20d). A stirred solution of acid **19d** (1.41 g, 8.38 mmol) and DMF (1 drop) in benzene (85 mL) was cooled in an ice–water bath. Oxalyl chloride (1.82 g, 14.3 mmol, 1.71 equiv) was added dropwise via syringe over 5 min. The mixture was removed from the cold bath and stirring continued at room temperature for 1 h. The mixture was concentrated by rotary evaporation leaving a yellow oil.

The crude acid chloride was dissolved in THF (85 mL). The solution was cooled to −78 °C and liquid ammonia condensed onto the reaction mixture for several minutes. After 30 min the mixture was warmed to room temperature under nitrogen pressure. The milky white mixture was poured into water (80 mL) and extracted with chloroform (5 × 80 mL). The combined organic layers were washed with saturated aqueous NaCl solution (100 mL), dried ($MgSO_4$), and concentrated to give 1.24 g (7.41 mmol, 89% from the acid) of a white solid. ^{1}H NMR (500 MHz, $CDCl_3$) δ 6.35 (dd, J = 17.6 Hz, J = 10.8 Hz, H_2C=CH), 5.8 (br s) and 5.5 (br s) (NH_2), 5.20 (d, J = 17.6 Hz, HHC=CH), 5.04 (d, J = 10.8 Hz, HHC=CH), 4.99 (s) and 4.96 (s) (CH_2=C), 2.22 (t, J = 7.6 Hz) and 2.20 (t, J = 7.9 Hz) (CCH_2 and CH_2CO), 1.65 (tt, J = 7.7 Hz, J = 7.7 Hz) and 1.51 (tt, J = 7.6 Hz, J = 7.6 Hz) (CCH_2CH_2 and CH_2CH_2CO), 1.37 (m, $CH_2CH_2CH_2CO$); ^{13}C NMR (125 MHz, $CDCl_3$) δ 175.65, 146.15, 138.82, 115.61, 113.10, 35.82, 31.06, 29.05, 27.72, 25.32; IR (KBr) 3300, 3195, 2940, 2864, 1662, 1635, 1594, 1417, 892 cm^{-1}; MS (EI) 167.1284 (167.1310 calcd for $C_{10}H_{17}NO$).

4-Methylenehex-5-enamide (20a). Prepared 3.11 g (24.8 mmol, 74% from the acid) following the above procedure. (TLC R_f 0.39 in EtOAc) ^{1}H NMR (500 MHz, $CDCl_3$) δ 6.38 (dd, J = 17.7 Hz, J = 10.9 Hz, H_2C=CH), 5.45 (br s, NH_2), 5.27 (d, J = 17.7 Hz, HHC=HC), 5.10 (d, J = 11.2 Hz, HHC=CH), 5.07 (s) and 5.04 (s) (CH_2=C), 2.58 (t, J = 7.7 Hz) and 2.43 (t, J = 7.8 Hz) (CH_2CH_2); ^{13}C NMR (125 MHz, $CDCl_3$) δ 174.66, 144.72, 138.22, 116.38, 113.73, 34.32, 26.81; IR (KBr) 3362, 3193, 3092, 2910, 1662, 1631, 1598, 1417, 1309, 1233, 1193, 984, 915, 895 cm^{-1}; MS (EI) 125.0828 (125.0841 calcd for $C_7H_{11}NO$).

5-Methylenehept-6-enamide (20b). Prepared 550 mg (3.95 mmol, 79% from the acid) after flash chromatography using EtOAc as eluant (TLC R_f 0.33). ^{1}H NMR (500 MHz, $CDCl_3$) δ 6.36 (dd, J = 17.6 Hz, J = 10.9 Hz, H_2C=CH), 5.4 (br s, NH_2), 5.25 (d, J = 17.6 Hz, HHC=CH), 5.07 (d, J = 10.6 Hz, HHC=CH), 5.04 (s) and 5.00 (s) (CH_2=C), 2.28 (t, J = 7.5 Hz) and 2.25 (t, J = 7.5 Hz) ($CH_2CH_2CH_2$), 1.86 (tt, J = 7.5 Hz, J = 7.5 Hz, $CH_2CH_2CH_2$); ^{13}C NMR (125 MHz, $CDCl_3$) δ 175.00, 145.33, 138.51, 116.25, 113.55, 35.19, 30.65, 23.66; IR (NaCl film) 3359, 3190, 2951, 2933, 1658, 1631, 1595, 1452, 1415, 1309, 893 cm^{-1}; MS (EI) 139.0989 (139.0997 calcd for $C_8H_{13}NO$).

6-Methyleneoct-7-enamide (20c). Prepared 1.45 g (9.46 mmol, 99% from the acid) following the above procedure. ^{1}H NMR (500 MHz, $CDCl_3$) δ 6.37 (dd, J = 17.7 Hz, J = 10.7 Hz, H_2C=CH) 5.42 (br s, NH_2), 5.22 (d, J = 17.6 Hz, HHC=CH), 5.06 (d, J = 10.6 Hz, HHC=CH), 5.02 (s) and 4.99 (s) (CH_2=C), 2.26 (t, J = 7.6 Hz) and 2.24 (t, J = 7.6 Hz) (CCH_2 and CH_2CO), 1.69 (m) and 1.56 (m) ($CH_2CH_2CH_2CH_2$); ^{13}C NMR (125 MHz, $CDCl_3$) δ 175.27, 145.88, 138.80, 115.91, 113.25, 35.77, 31.04, 27.65, 25.37; IR (KBr) 3367, 3194, 2844, 1662, 1635, 1595, 1419, 910, 895 cm^{-1}; MS (EI) 153.1143 (153.1154 calcd for $C_9H_{15}NO$).

Methyl (7-Methylenenon-8-enamido)hydroxyacetate (21d). A solution of amide **20d** (0.51 g, 3.05 mmol) and methyl glyoxalate (1.61 g, 18.3 mmol, 6.00 equiv, prepared immediately prior to the reaction and used without purification) in acetone (15 mL) was heated to reflux for 20 h. The mixture was poured into water (100 mL) and extracted with Et_2O (20 × 25 mL). The combined organic layers were dried ($MgSO_4$) and concentrated to give a white solid. Chromatography (1:1 hexane/EtOAc, R_f 0.17) gave 0.69 g (2.70 mmol, 89%) of a white solid. ^{1}H NMR (500 MHz, DMSO-d_6) δ 8.66 (d, J = 8.4 Hz, OH), 6.45 (d, J = 6.4 Hz, NH), 6.32 (dd, J = 17.6 Hz, J = 10.9 Hz, H_2C=CH), 5.43 (dd, J = 8.4 Hz, J = 6.4 Hz, CH(OH)), 5.20 (d, J = 17.6 Hz, HHC=CH), 5.03 (d, J = 10.8 Hz, HHC=CH), 4.99 (s) and 4.96 (s) (CH_2=C), 3.60 (s, OCH_3), 2.11 (t, J = 7.5 Hz) and 2.07 (t, J = 7.3 Hz) (CCH_2 and CH_2CO), 1.46 (tt, J = 7.5 Hz, J = 7.5 Hz) and 1.38 (tt, J = 7.6 Hz, J = 7.6 Hz) (CCH_2CH_2 and CH_2CH_2CO), 1.23 (tt, J = 7.5 Hz, J = 7.5 Hz, $CH_2CH_2CH_2CO$); ^{13}C NMR (125 MHz, DMSO-d_6) δ 172.56, 170.87, 146.27, 139.17, 116.41, 114.04, 71.32, 52.32, 35.38, 30.99, 28.88, 27.78, 25.22; IR (KBr) 3344, 3246, 3081, 2937, 2862, 1753, 1653, 1594, 1549, 1445, 1384, 1222, 1083, 963, 904, 891 cm^{-1}; MS (CI) 256.1539 (256.1549 calcd for $C_{13}H_{21}NO_4$ + H).

Methyl (4-Methylenehex-5-enamido)hydroxyacetate (21a). Prepared 1.00 g (4.69 mmol, 68%) as a white solid following the above procedure. ^{1}H NMR (500 MHz, DMSO-d_6) δ 8.76 (d, J = 8.4 Hz, OH), 6.50 (d, J = 6.4 Hz, NH), 6.33 (dd, J = 17.7 Hz, J = 10.9 Hz, H_2C=CH), 5.44 (dd, J = 8.4 Hz, J = 6.4 Hz, CH(OH)), 5.21 (d, J = 17.6 Hz, HHC=CH), 5.05 (d, J = 10.8 Hz, HHC=CH), 5.00 (s) and 4.97 (s) (CH_2=C), 3.61 (s, OCH_3), 2.35 (m) and 2.26 (m) (CH_2CH_2); ^{13}C NMR (125 MHz, DMSO-d_6) δ 171.99, 170.81, 145.25, 139.01, 116.59, 114.18, 71.39, 52.35, 33.89, 26.49; IR (KBr) 3402, 3332, 1753, 1741, 1658, 1541, 1360, 1252, 1105, 1078 cm^{-1}; MS (EI) 214.1091 (214.1079 calcd for $C_{10}H_{15}NO_4$).

Methyl (5-Methylenehept-6-enamido)hydroxyacetate (21b). Prepared 0.69 g (3.04 mmol, 77%) as a white solid following the above procedure. ^{1}H NMR (500 MHz, DMSO-d_6) δ 8.71 (d, J = 8.3 Hz, OH), 6.46 (d, J = 6.4 Hz, NH), 6.31 (dd, J = 17.7 Hz, J = 10.8 Hz, H_2C=CH), 5.43 (dd, J = 8.2 Hz, J = 6.6 Hz, CH(OH)), 5.22 (d, J = 17.1 Hz, HHC=CH), 5.04 (d, J = 11.1 Hz, HHC=CH), 5.00 (s) and 4.96 (s) (CH_2=C), 3.60 (s, OCH_3), 2.11 (t, J = 7.3 Hz, CCH_2), 2.11 (t, J = 7.3 Hz, CH_2CO), 1.61 (tt, J = 7.4 Hz, J = 7.4 Hz, $CH_2CH_2CH_2$); ^{13}C NMR (125 MHz, DMSO-d_6) δ 172.41, 170.87, 145.96, 139.01, 116.71, 114.24, 71.36, 52.34, 35.08, 30.54, 24.00; IR (KBr) 3344.6, 3326.0, 3087.4, 2956.9, 1751.0, 1653.8, 1551.2, 1456.0, 1446.8, 1437.5, 1364.8, 1226.9, 1105.7, 1079.6, 893.2 cm^{-1}; MS (EI) 227.1178 (227.1157 calcd for $C_{11}H_{17}NO_4$).

Methyl (6-Methyleneoct-7-enamido)hydroxyacetate (21c). Prepared 0.53 g (2.20 mmol, 91%) as a white solid following the above procedure. ^{1}H NMR (500 MHz, DMSO-d_6) δ 8.68 (d, J = 8.4 Hz, OH), 6.46 (d, J = 6.4 Hz, NH), 6.31 (dd, J = 17.6 Hz, J = 10.8 Hz, H_2C=CH), 5.42 (dd, J = 8.4 Hz, J = 6.4 Hz, CH(OH)), 5.20 (d, J = 17.7 Hz, HHC=CH), 5.03 (d, J = 10.8 Hz, HHC=CH), 4.99 (s) and 4.96 (s) (CH_2=C), 3.60 (s, OCH_3), 2.11 (t, J = 7.5 Hz) and 2.11 (t, J = 7.3 Hz) (CCH_2 and CH_2CO), 1.47 (tt, J = 7.5 Hz, J = 7.5 Hz) and 1.37 (tt, J = 7.5 Hz, J = 7.5 Hz) ($CH_2CH_2CH_2CO$); ^{13}C NMR (125 MHz, DMSO-d_6) δ 172.56, 170.90, 146.23, 139.15, 116.47, 114.16, 71.35, 52.36, 35.24, 30.85, 27.52, 25.30; IR (KBr) 3334.7, 3236.0, 2938.7, 1750.1, 1653.9, 1550.6, 1446.4, 1364.7, 1225.4, 1103.5, 1083.0 cm^{-1}; MS (CI) 242.1363 (242.1392 calcd for $C_{12}H_{19}NO_4$ + H).

Methyl (7-Methylenenon-8-enamido)(acetyloxy)acetate (22d). A solution of alcohol **21d** (0.69 g, 2.70 mmol) and pyridine (4 drops) in acetic anhydride (6 mL) was stirred at room temperature under nitrogen pressure for 22 h. The mixture was concentrated leaving a yellow oil. The oil was dissolved in chloroform (40 mL) and washed with water (30 mL) and saturated aqueous NaCl solution (30 mL). The organic phase was dried ($MgSO_4$) and concentrated to give a yellow oil. Chromatography (2:1 hexane/EtOAc, R_f 0.23) afforded 0.76 g (2.56 mmol, 95%) of a colorless oil. ^{1}H NMR (500 MHz, $CDCl_3$) δ 6.79 (d, J = 8.7 Hz, NH), 6.38 (d, J = 9.0 Hz, CH(OAc)), 6.35 (dd, J = 18.2 Hz, J = 11.1 Hz, H_2C=CH), 5.20 (d, J = 17.4 Hz, HHC=CH), 5.04 (d, J = 10.8 Hz, HHC=CH), 5.00 (s) and 4.97 (s) (CH_2=C), 3.81 (s, CO_2CH_3), 2.27 (t, J = 7.8 Hz) and 2.20 (t, J = 7.6 Hz) (CCH_2 and CH_2CO), 2.11 (s, $COCH_3$), 1.68 (tt, J = 7.7 Hz, J = 7.7 Hz) and 1.50 (tt, J = 7.6 Hz, J = 7.6 Hz) (CCH_2CH_2 and CH_2CH_2CO), 1.36 (m, $CH_2CH_2CH_2CO$); ^{13}C NMR (125 MHz, $CDCl_3$) δ 172.72, 170.49, 167.28, 146.13, 138.84, 115.67, 113.15, 72.18, 53.31, 36.15, 31.08, 28.97, 27.70, 24.91, 20.65; IR (film) 3304, 2937, 2862, 1752, 1700, 1676, 1595, 1533, 1439, 1374, 1341, 1218, 1160, 1041, 900 cm^{-1}; MS (CI) 298.1661 (0.6%) (298.1654 calcd for $C_{15}H_{23}NO_5$ + H), 238.1457 (100%) (238.1443 calcd for $C_{13}H_{19}NO_3$ + H (MH^+ − HOAc)).

Methyl (4-Methylenehex-5-enamido)(acetyloxy)acetate (22a). Prepared 0.96 g (3.76 mmol, 80%) as a colorless oil after chromatography in 1:1 petroleum/Et_2O (R_f 0.18). ^{1}H NMR (500 MHz, $CDCl_3$) δ 6.82 (br d, J = 8.8 Hz, NH), 6.38 (d, J = 9.1 Hz, CH(OAc)), 6.36 (dd, J = 17.6 Hz, J = 10.9 Hz, H_2C=CH), 5.25 (d, J = 17.7 Hz, HHC=CH), 5.10 (d, J = 10.9 Hz, HHC=CH), 5.05 (s) and 5.01 (s) (CH_2=C), 3.80 (s, CO_2CH_3), 2.59 (t, J = 7.7 Hz) and 2.47 (m) (CH_2CH_2CO), 2.11 (s, $COCH_3$); ^{13}C NMR (125 MHz, $CDCl_3$) δ 172.13, 170.44, 167.22, 144.41, 138.08, 116.50, 113.84, 72.13, 53.33, 34.70, 26.47, 20.65; IR (film) 3313, 2958, 1752, 1695, 1683, 1677, 1597, 1533, 1439, 1375, 1330, 1219, 1171, 1040, 959, 906 cm^{-1}; MS (CI, methane) 256.1203 (256.1185 calcd for $C_{12}H_{17}NO_5$ + H).

Methyl (5-Methylenehept-6-enamido)(acetyloxy)acetate (22b). Prepared 653 mg (2.43 mmol, 80%) as a pale-yellow oil after chromatography in 1:1 petroleum/Et_2O (R_f 0.14). ^1H NMR (500 MHz, $CDCl_3$) δ 6.78 (br d, J = 8.8 Hz, NH), 6.38 (d, J = 9.1 Hz, C*H*(OAc)), 6.35 (dd, J = 16.9 Hz, J = 10.9 Hz, H_2C=C*H*), 5.23 (d, J = 17.6 Hz, *H*HC=CH), 5.07 (d, J = 11.3 Hz, H*H*C=CH), 5.04 (s) and 4.99 (s) (CH_2=C), 3.81 (s, CO_2CH_3), 2.29 (t, J = 7.5 Hz) and 2.26 (t, J = 7.3 Hz) (CH_2 and CH_2CO), 2.11 (s, $COCH_3$), 1.86 (tt, J = 7.4 Hz, J = 7.4 Hz, CH_2CH$_2$CO); ^{13}C NMR (125 MHz, $CDCl_3$) δ 172.47, 170.48, 167.26, 145.16, 138.42, 116.43, 113.62, 72.16, 53.32, 35.50, 30.51, 23.27, 20.65; IR (film) 3312, 2957, 1755, 1677, 1596, 1531, 1439, 1376, 1222, 1165, 1041, 903, 757 cm^{-1}; MS (CI) 270.1365 (1.3%) (270.1341 calcd for $C_{13}H_{19}NO_5$ + H).

Methyl (6-Methyleneoct-7-enamido)(acetyloxy)acetate (22c). Prepared 0.53 g (1.87 mmol, 85%) as a colorless oil by the above procedure (TLC R_f 0.22 in 1:1 petroleum ether/Et_2O). ^1H NMR (500 MHz, $CDCl_3$) δ 6.84 (d, J = 8.8 Hz, NH), 6.38 (d, J = 9.1 Hz, C*H*(OAc)), 6.36 (dd, J = 17.6 Hz, J = 10.9 Hz, H_2C=C*H*), 5.21 (d, J = 17.6 Hz, *H*HC=CH), 5.05 (d, J = 10.9 Hz, H*H*C=CH), 5.05 (s) and 4.98 (s) (CH_2=C), 3.81 (s, CO_2CH_3), 2.29 (dt, J = 7.5 Hz, J = 1.4 Hz) and 2.23 (t, J = 7.6 Hz) (CH_2 and CH_2CO), 2.11 (s, $COCH_3$), 1.70 (m) and 1.53 (m) (CH_2CH_2CH$_2$CO); ^{13}C NMR (125 MHz, $CDCl_3$) δ 172.63, 170.46, 167.26, 145.76, 138.72, 115.88, 113.21, 72.16, 53.29, 36.03, 30.94, 27.49, 24.92, 20.64; IR (film) 3305, 2952, 1753, 1676, 1529, 1439, 1375, 1220, 1161, 1039, 958, 904 cm^{-1}; MS (CI) 284.1487 (0.7%) (284.1498 calcd for $C_{14}H_{21}NO_5$ + H), 224.1265 (100%) (224.1987 calcd for $C_{12}H_{17}NO_3$ + H (MH^+ - HOAc)).

Solution-Phase Diels–Alder Cycloadditions. Thermolyses were conducted in sealed vessels. Samples were degassed by successive freeze–pum–thaw cycles using a medium-vacuum oil diffusion pump. Crude product mixtures in xylenes solvent were loaded directly onto silica gel; the column was washed with three volumes of hexane prior to elution with a hexane/EtOAc mixture.

2-Carbomethoxy-8-oxo-1-azabicyclo[3.3.1]non-4-ene (3). A solution of acetate **22a** (140 mg, 548 μmol) in xylenes (56 mL) was heated to 252 °C for 2.50 min. Chromatography (1:1 hexane/EtOAc, R_f 0.33) afforded 31.2 mg (160 μmol, 29%) of a colorless oil which crystallized on standing. ^1H NMR (500 MHz, C_6D_6) δ 5.07 (ddd, J = 7.3 Hz, J = 6.0 Hz, J = 1.3 Hz, *H*C=C), 4.46 (ddd, J = 8.1 Hz, J = 6.8 Hz, J = 1.4 Hz, C*H*(CO_2CH_3)), 3.25 (s, CO_2CH_3), 3.08 (ddd, J = 12.9 Hz, J = 1.6 Hz, J = 1.6 Hz) and 3.00 (d, J = 13.0 Hz, CCH_2N), 2.51 (ddd, J = 15.0 Hz, J = 10.3 Hz, J = 7.4 Hz, C*H*HCO), 2.33 (dd, J = 15.1 Hz, J = 7.1 Hz, C*H*HCH(CO_2CH_3)), 2.27 (dd, J = 15.0 Hz, J = 8.2 Hz, CH*H*CO), 2.21 (dddd, J = 15.1 Hz, J = 8.2 Hz, J = 2.5 Hz, CH*H*CH(CO_2CH_3)), 1.98 (dd, J = 11.4 Hz, J = 10.3 Hz) and 1.86 (m) (CCH_2); ^{13}C NMR (125 MHz, C_6D_6) δ 182.71, 172.12, 151.95, 123.63, 58.71, 51.50, 47.72, 38.97, 30.81, 29.59; IR (C_6D_6) 2952.48, 1751.05, 1702.84, 1315.21, 1216.86, 1197.58, 1166.72, 1151.29, 1106.94, 1020.16 cm^{-1}; MS (EI) 195.0889 (195.0895 calcd for $C_{10}H_{13}NO_3$).

9-Carbomethoxy-2-oxo-1-azabicyclo[4.3.1]dec-6-ene (4). A solution of acetate **22b** (100 mg, 371 μmol) in xylenes (37 mL) was heated to 200 °C for 2.0 h. Chromatogapghy (Et_2O, R_f 0.38) afforded 63.4 mg (303 μmol, 82%) of a colorless oil which crystallized slowly upon standing. ^1H NMR (500 MHz, C_6D_6) δ 5.02 (ddd, J = 7.3 Hz, J = 4.1 Hz, J = 1.7 Hz, *H*C=C), 4.94 (ddd, J = 8.5 Hz, J = 7.5 Hz, J = 1.7 Hz, C*H*-(CO_2CH_3)), 3.28 (s, CO_2CH_3), 3.26 (ddd, J = 14.5 Hz, J = 1.7 Hz, J = 1.7 Hz) and 3.00 (d, J = 14.5 Hz) (CCH_2N), 2.45 (ddd, J = 13.3 Hz, J = 13.0 Hz, J = 3.0 Hz, C*H*HCO), 2.27 (ddd, J = 15.4 Hz, J = 7.5 Hz, J = 7.3 Hz, C*H*HCH(CO_2CH_3)), 2.21 (ddd, J = 13.0 Hz, J = 4.6 Hz, J = 2.8 Hz, CH*H*CO), 2.04 (dddd, J = 15.4 Hz, J = 8.5 Hz, J = 4.1 Hz, J = 1.9 Hz, CH*H*CH(CO_2CH_3)), 1.91 (dd, J = 12.1 Hz, J = 6.3 Hz) and 1.69 (dddd, J = 12.1 Hz, J = 12.0 Hz, J = 5.8 Hz, J = 1.9 Hz) (CCH_2), 1.49 (dddd, J = 14.0 Hz, J = 5.8 Hz, J = 4.6 Hz, J = 3.0 Hz) and 1.31 (ddddd, J = 14.0 Hz, J = 13.3 Hz, J = 12.0 Hz, J = 6.3 Hz, J = 2.8 Hz) (CH_2CH$_2$CO); ^{13}C NMR (125 MHz, C_6D_6) δ 180.84 (C_2), 172.96 (C_{11}), 148.77 (C_6), 118.61 (C_7), 53.88 (C_9), 51.51 (C_{12}), 48.22 (C_{10}), 36.01 (C_3), 34.35 (C_5), 31.56 (C_4), 27.36 (C_8); IR (KBr) 3035.5, 2951.5, 2923.4, 2854.7, 1733.8, 1660.0, 1456.2, 1430.7, 1384.8, 1367.0, 1224.4, 1160.7, 1018.0 cm^{-1}; MS (EI) 209.1050 (209.1052 calcd for $C_{11}H_{15}NO_3$).

10-Carbomethoxy-2-oxo-1-azabicyclo[5.3.1]undec-7-ene (5). A solution of acetate **22c** (100 mg, 353 μmol) in xylenes (35 mL) was heated to 215 °C for 2.0 h. Chromatography (Et_2O) afforded 60 mg (269 μmol, 76%) of a colorless crystalline solid. ^1H NMR (500 MHz, C_6D_6) δ 5.37 (ddd, J = 9.1 Hz, J = 7.7 Hz, J = 1.7 Hz, C*H*(CO_2CH_3)), 5.10 (ddd, J = 9.3 Hz, J = 4.6 Hz, J = 2.3 Hz, *H*C=C), 3.41 (ddd, J = 15.3 Hz, J = 1.6 Hz, J = 1.6 Hz, CC*H*HN), 3.29 (s, CO_2CH_3), 3.03 (ddd, J = 15.4 Hz, J = 3.3 Hz, J = 1.6 Hz, CCH*H*N), 2.48 (dd, J = 13.3 Hz, J = 9.3 Hz, C*H*HCO), 2.39 (ddd, J = 16.1 Hz, J = 8.9 Hz, J = 7.2 Hz) and 2.15 (dddddd, J = 16.0 Hz, J = 7.9 Hz, J = 4.8 Hz, J = 3.1 Hz, J = 1.6 Hz, J = 0.6 Hz) (CH_2CH(CO_2CH_3)), 1.95 (m, CH*H*CO and CC*H*H), 1.66 (ddd, J = 14.8 Hz, J = 11.9 Hz, J = 6.2 Hz, CCH*H*), 1.51 (m, C*H*HCH$_2$CO), 1.43 (dddd, J = 14.8 Hz, J = 7.6 Hz, J = 5.9 Hz, J = 1.7 Hz, CCH$_2$C*H*H), 1.13 (dddd, J = 14.5 Hz, J = 11.7 Hz, J = 11.7 Hz, J = 6.3 Hz, CCH$_2$CH*H*), 1.05 (ddd, J = 14.6 Hz, J = 10.9 Hz, J = 10.9 Hz, CH*H*CH$_2$CO); ^{13}C NMR (125 MHz, C_6D_6) δ 177.35 (C_2), 173.09 (C_{12}), 145.05 (C_7), 122.35 (C_8), 52.03 (C_{10}), 51.53 (C_{13}), 42.84 (C_{11}), 37.90 (C_3), 33.37 (C_6), 27.70 (C_5), 26.66 (C_9), 23.99 (C_4); IR (KBr) 3038, 2965, 2936, 2898, 2853, 1747, 1645, 1406, 1364, 1307, 1244, 1208, 1166, 1150, 1056, 1021, 801, 793, 733 cm^{-1}; MS (EI) 223.1208 (223.1208 calcd for $C_{12}H_{17}NO_3$).

11-Carbomethoxy-2-oxo-1-azabicyclo[6.3.1]dodec-8-ene (6). A solution of acetate **22d** (206 mg, 692 μmol) in xylenes (69 mL) was heated to 307 °C for 5.0 min. Chromatography (2:1 hexane/EtOAc) afforded 14.1 mg (59.4 μmol, 9%) of a colorless amorphous solid. ^1H NMR (500 MHz, C_6D_6) δ 5.13 (m, *H*C=CC), 5.08 (dd, J = 8.9 Hz, J = 8.9 Hz, C*H*(CO_2CH_3)), 3.65 (d, J = 15.5 Hz, CC*H*HN), 3.31 (s, CO_2CH_3), 3.17 (d, J = 15.4 Hz, CCH*H*N), 2.41 (dd, J = 15.8 Hz, J = 7.8 Hz, 1 H), 2.39 (ddd, J = 17.7 Hz, J = 9.1 Hz, J = 6.1 Hz, 1 H), 2.09 (m, 2 H), 1.88 (m, 2 H), 1.63 (ddd, J = 13.8 Hz, J = 13.8 Hz, J = 5.1 Hz, 1 H), 1.27 (m, 3 H), 1.13 (m, 1 H), 0.88 (m, 1 H), 0.73 (m, 1 H); ^{13}C NMR (125 MHz, C_6D_6) δ 173.71 (C_2), 172.78 (C_{13}), 143.65 (C_8), 123.55 (C_9), 52.29 (C_{11}), 51.56 (C_{14}), 42.67 (C_{12}), 33.43, 29.49, 26.89, 26.33, 21.25, 20.94; IR (NaCl film) 2935, 1745, 1641, 1462, 1454, 1435, 1406, 1273, 1228, 1198, 1169, 1059, 1038, 1014, 995, 956 cm^{-1}; MS (EI) 237.1366 (237.1365 calcd for $C_{13}H_{19}NO_3$).

1-Aza-2-carbomethoxy-4-ethenyl-10-oxocyclodec-4-ene (34). Also isolated from the thermolysis of **22d** was 40.8 mg (172 μmol, 25%) of a colorless amorphous solid. ^1H NMR (500 MHz, DMSO-d_6, 150 °C) δ 7.4 (br s, NH), 6.38 (dd, J = 17.6 Hz, J = 10.9 Hz, H_2C=C*H*), 5.72 (dd, J = 9.8 Hz, J = 6.7 Hz, C=C*H*), 5.22 (d, J = 17.6 Hz, *H*HC=CH), 5.03 (d, J = 10.9 Hz, H*H*C=CH), 4.37 (ddd, J = 8.4 Hz, J = 8.4 Hz, J = 4.3 Hz, C*H*(CO_2Me)), 3.80 (s, CO_2CH_3), 2.94 (dd, J = 13.8 Hz, J = 8.5 Hz) and 2.84 (dd, J = 13.9 Hz, J = 4.3 Hz) (CHCH_2C), 2.48 (m, C=CHC*H*H), 2.24 (m, C=CHCH*H* and $COCH_2$), 1.82 (m, CH_2CH$_2$CH$_2$CO); ^1H NMR (500 MHz, $CDCl_3$, -25 °C) δ 6.28 (dd, J = 17.6 Hz, J = 11.0 Hz, H_2C=C*H*), 6.21 (d, J = 8.8 Hz, NH), 5.66 (dd, J = 12.4 Hz, J = 3.9 Hz, C=C*H*), 4.97 (d, J = 17.5 Hz, *H*HC=CH), 4.88 (d, J = 11.0 Hz, H*H*C=CH), 4.84 (ddd, J = 16.9 Hz, J = 8.7 Hz, J = 1.7 Hz, C*H*(CO_2Me)), 3.69 (s, CO_2CH_3), 3.14 (dd, J = 14.4 Hz, J = 6.6 Hz) and 2.70 (dd, J = 14.3 Hz, J = 1.3 Hz) (CHCH_2C), 2.52 (ddd, J = 15.9 Hz, J = 14.7 Hz, J = 2.8 Hz, COC*H*H), 2.31 (dddd, J = 15.4 Hz, J = 11.9 Hz, J = 11.9 Hz, J = 3.6 Hz, C=CHC*H*H), 2.1 (m, COCH*H* and C=CHCH*H*), 1.75 (m, CH_2CH_2CH$_2$CO); ^{13}C NMR (125 MHz, DMSO-d_6, 150 °C) δ 172.71, 170.47, 139.58, 135.96, 132.90, 109.41, 50.77, 50.44, 35.86, 26.96, 25.54, 25.36, 23.71; ^{13}C NMR (125 MHz, $CDCl_3$, -25 °C) δ 174.15, 171.99, 140.12 (H_2C=*C*H), 138.81 (C_5), 132.30 (C_4), 110.31 (H_2C=CH), 52.50 (OCH_3), 49.38 (C_2), 36.83 (C_9), 28.00, 26.13 (C_6), 24.98 (C_3), 24.40; IR (KBr) 3311, 1730, 1639, 1549, 1460, 1267, 1232, 1217, 1194, 1093, 1070 cm^{-1}; MS (EI) 237.1355 (237.1365 calcd for $C_{13}H_{19}NO_3$).

2-Carbomethoxy-8-oxo-1-aza-4,5-epoxybicyclo[3.3.1]nonane (30). A sample of **3** (10.9 mg, 55.8 μmol) was exposed to air for 1 h. Chromatography (1:1 hexane/Et_2O) afforded 5.0 mg (23.7 μmol, 42%) of a colorless amorphous solid. ^1H NMR (500 MHz, C_6D_6) δ 4.87 (ddd, J = 9.9 Hz, J = 7.9 Hz, J = 1.6 Hz, C*H*(CO_2CH_3)), 3.19 (s, CO_2CH_3), 2.91 (d, J = 13.8 Hz) and 2.40 (dd, J = 13.8 Hz, J = 2.1 Hz) (CCH_2N), 2.08 (m, CH_2C=O), 1.99 (dd, J = 6.1 Hz, J = 6.1 Hz, CH(O)C), 1.92 (ddd, J = 14.5 Hz, J = 7.3 Hz, J = 7.2 Hz, CHC*H*HCH), 1.70 (dd, J = 11.0 Hz, J = 11.0 Hz, CC*H*H), 1.42 (ddd, J = 14.8 Hz, J = 9.9 Hz, J = 5.7 Hz, CHCH*H*CH), 0.89 (dddd, J = 11.9 Hz, J = 8.3 Hz, J = 8.3 Hz, J = 2.2 Hz, CCH*H*); ^{13}C NMR (125 MHz, C_6D_6) δ 181.73, 172.30, 62.53, 56.03, 54.09, 52.00, 49.32, 32.27, 28.41, 26.41; MS (EI) 211.0836 (211.0844 calcd for $C_{10}H_{13}NO_4$).

2-Carboxy-8-oxo-1-azabicyclo[3.3.1]non-4-ene (33). To a solution of **3** (55.7 mg, 285 μmol) in acetonitrile (6 mL) was added a solution of lithium hydroxide (61.3 mg, 1.46 mmol, 5.13 equiv) in water (5 mL). After 1.0 h the mixture was diluted with saturated aqueous $NaHCO_3$ solution (50 mL) and $CHCl_3$ (25 mL). The aqueous phase was adjusted to pH 4.97 with 2 M HCl and then extracted with $CHCl_3$ (5 × 25 mL). A mixture of the aqueous phase and $CHCl_3$ (25 mL) was then acidified to pH 2.01 and extracted with $CHCl_3$ (12 × 25 mL). The combined pH 2 extracts were dried ($MgSO_4$) and concentrated to give 24.0 mg (132 μmol, 46%) of a colorless solid. ^1H NMR (500 MHz, $CDCl_3$) δ 5.65 (dd, J = 6.4 Hz, J = 6.4 Hz, *H*C=C), 4.37 (dd, J = 7.6 Hz, J = 7.6 Hz, C*H*(CO_2CH_3)), 3.79 (d, J = 12.8 Hz, CC*H*HN), 3.30 (ddd, J = 15.1 Hz, J = 10.4 Hz, J = 7.2 Hz, 1 H), 3.20 (d, J = 12.8 Hz, CCH*H*N), 2.90 (m, 2 H), 2.71 (dd, J = 15.1 Hz, J = 8.3 Hz, 1 H), 2.52 (m, 2 H); ^{13}C NMR (125 MHz, $CDCl_3$) δ 184.45, 175.66, 151.78, 124.35, 59.06, 48.08, 38.83, 30.68, 29.83; IR (KBr) 3446.17, 2925.48, 2854.13, 1716.34,

1635.34, 1417.42, 1270.86 cm^{-1}; MS (CI) 182 (MH$^+$).

Acknowledgment. We are grateful to the National Science Foundation (Chemistry Division) for financial support of this work. We also wish to thank Dr. Joseph Ziller for his assistance with the X-ray crystallography.

Supplementary Material Available: Description of X-ray diffraction experiments, tables of structure determination data, atomic coordinates, displacement coordinates, and interatomic distances and angles for **4** and **5**, and ORTEP drawings of **4** and **5** (12 pages). Ordering information is given on any current masthead page.

Synthesis and Use of Glycosyl Phosphites: An Effective Route to Glycosyl Phosphates, Sugar Nucleotides, and Glycosides

Mui Mui Sim,† Hirosato Kondo, and Chi-Huey Wong*

Contribution from the Department of Chemistry, The Scripps Research Institute, 10666 North Torrey Pines Road, La Jolla, California 92037. *Received August 6, 1992*

Abstract: An efficient and convenient synthetic route to glycosyl phosphites and phosphates has been developed that uses dibenzyl *N,N*-diethylphosphoramidite as a phosphitylating reagent. Glycosyl phosphites and phosphates of 2-acetamido-2-deoxy-D-galactose (GalNAc) (**29**), 2-acetamido-2-deoxy-D-glucose (GlcNAc) (**30**), D-galactose (Gal) (**31**), D-glucose (Glc) (**32**), D-mannose (Man) (**33**), L-rhamnose (Rha) (**34**), L-fucose (Fuc) (**35**), and *N*-acetylneuraminic acid (NeuAc) (**41**) were prepared by this procedure. Compounds **29** and **30** were obtained as α anomers exclusively, whereas compounds **31**, **32**, and **41** were obtained as β anomers, and compounds **33** and **34**, as α anomers, predominately. The phosphates are useful for the synthesis of sugar nucleotides, and the phosphites are effective glycosylation reagents.

Introduction

We report here the use of dibenzyl *N,N*-diethylphosphoramidite (DDP) in the preparation of dibenzyl glycosyl phosphites, which can be easily converted to glycosyl phosphates or used as glycosylation reagents in oligosaccharide synthesis (Scheme I). Glycosyl phosphates are key intermediates in the biosynthesis of carbohydrates.[1] In the Lenoir pathway,[2] sugar is initially activated as a sugar-1-phosphate and transformed into a nucleoside diphosphate sugar, which then functions as a donor substrate for a glycosyltransferase-catalyzed transfer of the sugar moiety to a glycosyl acceptor.

Due to the growing interest in enzymatic oligosaccharide synthesis, the availability of sugar nucleotides has become a subject for investigation. Several enzymatic[3-6] and chemical[7-12] methods for the synthesis of sugar nucleotides have been reported. These methods usually start with glycosyl 1-phosphates, which are generally quite expensive and not all commercially available.

Many elegant and new methods for the synthesis of glycosyl phosphates, either enzymatic[6a,f,13] or chemical,[8,11,12,14-19] have been developed. We have recently reported[12a] the use of DDP in the synthesis of β-L-fucosyl dibenzyl phosphite, which is further converted to fucosyl phosphate and GDP-fucose. To investigate the generality of this phosphitylation reaction, we have carried out the synthesis of glycosyl phosphites of seven important sugars, including GalNAc, GlcNAc, Gal, Glc, Man, Rha, and NeuAc, and conversion of the phosphites to phosphates (Schemes II-IV). The glycosyl phosphites can also be used as glycosylation reagents, as illustrated in the synthesis of α-2,3- and α-2,6-linked sialosides (Scheme V).[12b] The sialyl phosphite is a very effective sialylation reagent,[12b,c] giving the α-2,3- or α-2,6-linked sialosides in 30-80% yield, which is higher than or comparable to that from reactions based on other sialylation reagents.[20,21]

Results and Discussion

Glycosyl Phosphites and Phosphates. The phosphitylating reagent DDP was first introduced in 1980 by Smirnova et al.[22] and was subsequently used by others[23] for phosphorylating alcohols. However, it was only recently that the phosphitylating reagent was characterized.[24]

We chose DDP to prepare the glycosyl phosphates for the following reasons: it is relatively cheap and easy to prepare on

† On study leave from the Institute of Molecular and Cell Biology, National University of Singapore.

(1) Kennedy, J. F.; White, C. A. *Bioactive Carbohydrates*; Wiley: New York, 1983; Chapter 5, p 98.
(2) (a) Caputto, R.; Leloir, L. F.; Cardini, C. E.; Paladini, A. C. *J. Biol. Chem.* **1950**, *184*, 333. (b) Watkins, W. M. *Carbohydr. Res.* **1986**, *149*, 1.
(3) (a) Ginsburg, V. *Adv. Enzymol. Relat. Subj. Biochem.* **1964**, *26*, 35. (b) Simon, E. S.; Granbowski, S.; Whitesides, G. M. *J. Org. Chem.* **1990**, *55*, 1834. (c) Heidlas, J. E.; Lees, W. J.; Pale, P.; Whitesides, G. M. *J. Org. Chem.* **1992**, *57*, 146.
(4) Korf, U.; Thimm, J.; Thiem, J. *Synlett* **1991**, 313.
(5) (a) Ginsburg, V. *J. Biol. Chem.* **1960**, *235*, 2196. (b) Yamamoto, K.; Maruyama, T.; Kumagai, H.; Tochikura, T. *Agric. Biol. Chem.* **1984**, *48*, 823.
(6) (a) Ishihara, H.; Massaro, D. J.; Heath, E. C. *J. Biol. Chem.* **1968**, *243*, 1103. (b) Ishihara, H.; Heath, E. C. *J. Biol. Chem.* **1968**, *243*, 1110. (c) Schachter, H.; Ishihara, H.; Heath, E. C. *Methods Enzymol.* **1972**, *28*, 285. (d) Richard, W. L.; Serif, G. S. *Biochim. Biophys. Acta* **1977**, *484*, 353. (e) Kilker, R. D.; Shuey, D. K.; Serif, G. S. *Biochim. Biophys. Acta* **1979**, *570*, 271. (f) Butler, W.; Serif, G. S. *Biochim. Biophys. Acta* **1985**, *829*, 238.
(7) (a) Kochetkov, N. K.; Shibaev, V. N. *Adv. Carbohydr. Chem. Biochem.* **1973**, *28*, 307. (b) Moffat, J. G. *Methods Enzymol.* **1966**, *8*, 136. (c) Roseman, S.; Distler, J. J.; Moffat, J. G.; Khoran, H. G. *J. Am. Chem. Soc.* **1961**, *83*, 659.
(8) Nunez, H. A.; O'Connor, J. V.; Rosevear, P. R.; Baker, R. *Can. J. Chem.* **1981**, *59*, 2086.
(9) Rajan, V. P.; Larsen, R. D.; Ajmera, S.; Emet, L. K.; Lowe, J. B. *J. Biol. Chem.* **1989**, *264*, 11158.
(10) Gokhale, U. B.; Hindsgaul, O.; Palacic, M. M. *Can. J. Chem.* **1990**, *68*, 1063.
(11) Schmidt, R. R.; Wegmann, B.; Jung, K.-H. *Liebigs Ann. Chem.* **1991**, *191*, 121.
(12) (a) Ichikawa, Y.; Sim, M. M.; Wong, C.-H. *J. Org. Chem.* **1992**, *57*, 2943. (b) For a preliminary study on the use of dibenzyl sialyl phosphite in sialylation, see: Kondo, H.; Ichikawa, Y.; Wong, C.-H. *J. Am. Chem. Soc.* **1992**, *114*, 8748. (c) For sialylation with diethyl sialyl phosphite, see: Martin, T. J.; Schmidt, R. R. *Tetrahedron Lett.* **1992**, *33*, 6123.
(13) Fessner, W.-D.; Eyrisch, O. *Angew. Chem., Int. Ed. Engl.* **1992**, *31* (1), 56.
(14) Prihar, H. S.; Behrman, E. J. *Biochemistry* **1973**, *12*, 997.
(15) (a) Westerduin, P.; Veeneman, G. H.; Magrugg, J. E.; van der Marel, G. A.; van Boom, J. H. *Tetrahedron Lett.* **1986**, *27* (10), 1211. (b) Westerduin, P.; Veeneman, G. H.; Marugg, J. E.; van der Marel, G. A.; van Boom, J. H. *Tetrahedron Lett.* **1986**, *27* (51), 6271.
(16) Roy, R.; Tropper, F. D.; Graud-Maites, C. *Can. J. Chem.* **1991**, *69*, 1462.
(17) Veeneman, G. H.; Broxterman, H. J. G.; van der Marel, G. A.; van Boom, J. H. *Tetrahedron Lett.* **1991**, *32* (43), 6175.
(18) Inage, M.; Chaki, H.; Kusumoto, S.; Shiba, T. *Chem. Lett.* **1982**, 1281.
(19) Sabesan, S.; Neira, S. *Carbohydr. Res.* **1992**, *223*, 169.

0002-7863/93/1515-2260$04.00/0